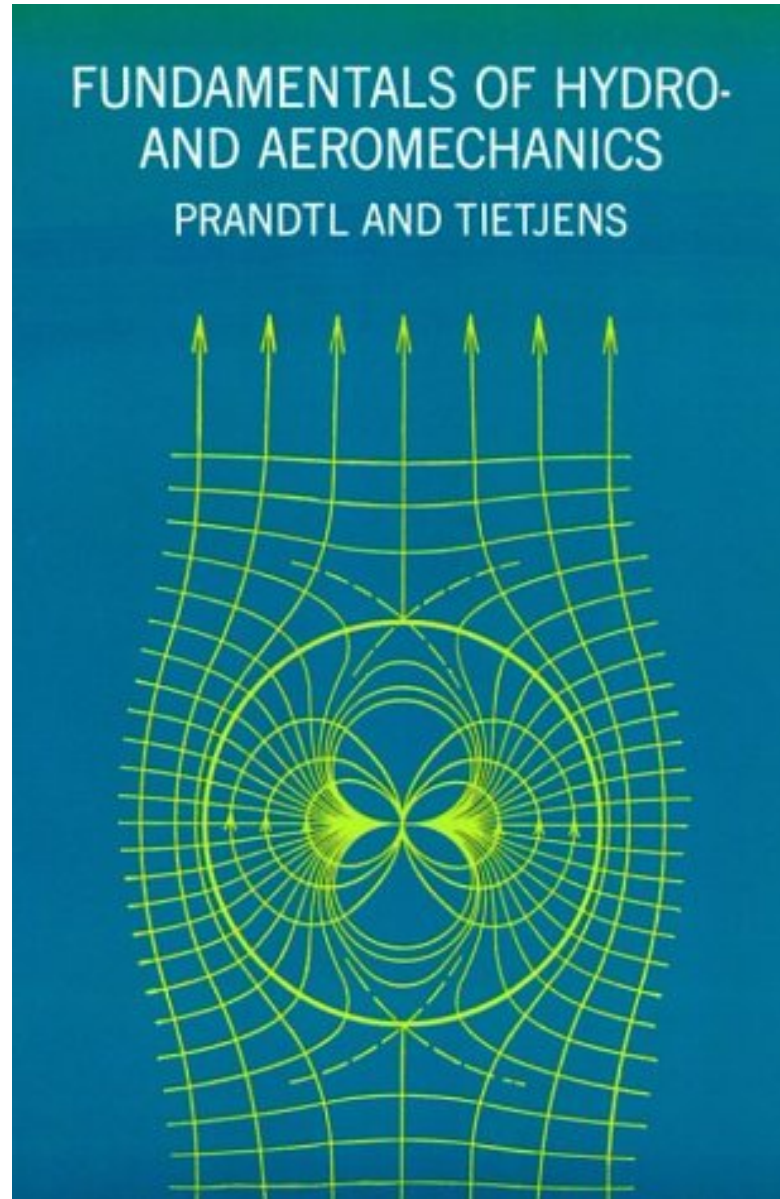


# AA200 Applied Aerodynamics

## Chapter 11 - Two-dimensional airfoil theory

Brian Cantwell  
Department of Aeronautics and Astronautics  
Stanford University

Potential flow over a circle - lines of constant  
velocity potential  $\Phi$  and stream function  $\Psi$



## 11.1 Creation of circulation over an airfoil

$$\frac{\bar{F}}{\rho(\text{one unit of span})} = \frac{d}{dt} \int_{A_w} \Phi \hat{n} dl - \bar{U}_\infty(t) \times \Gamma(t) \hat{k} \quad (11.1)$$

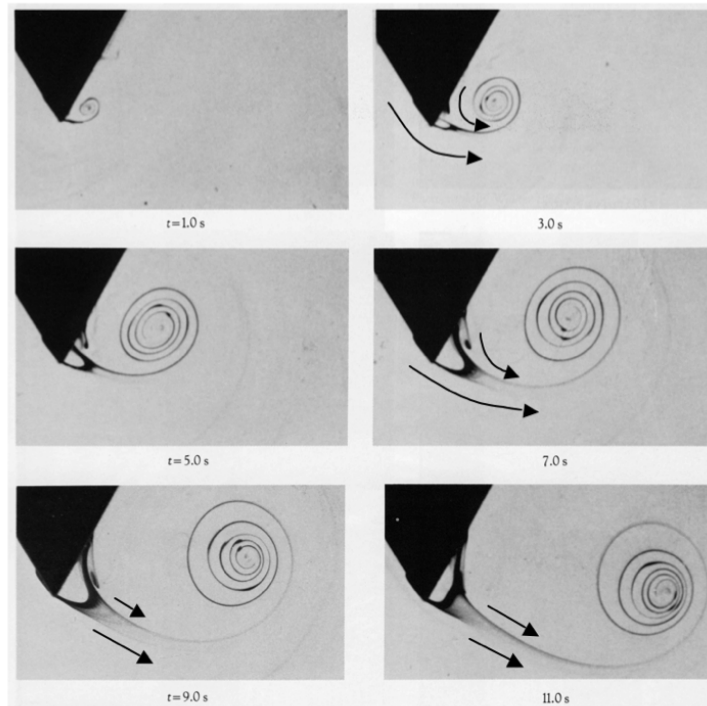


*Figure 11.1 Starting vortex formation about a corner in an impulsively started incompressible fluid.*

## Recall the solution for a point vortex

### 5) Point vortex

Here we solve the Poisson equation for the stream function with a point source of circulation at the origin.

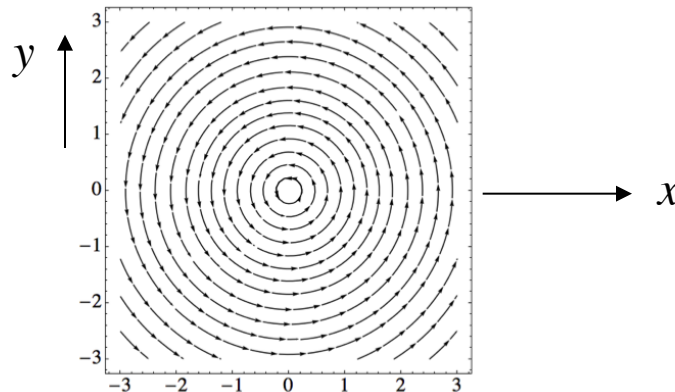
$$\nabla^2 \Psi = -\Gamma \delta(\bar{x}) \quad (10.93)$$

where  $\Gamma$  is the strength of the source. The Greens function solution is

$$\Psi(\bar{x}) = \frac{-1}{2\pi} \int_A \Gamma \delta(\bar{x}_s) \text{Ln}(|\bar{x} - \bar{x}_s|) dA = \frac{-1}{2\pi} \int_0^{2\pi} \int_0^r \Gamma \delta(r_s) \text{Ln}(|r - r_s|) dr d\theta = \frac{-\Gamma}{2\pi} \text{Ln}(r) \quad (10.94)$$

This is the same solution we derived earlier through a limiting process of allowing a finite vortex line become infinite. The potentials for a point vortex are

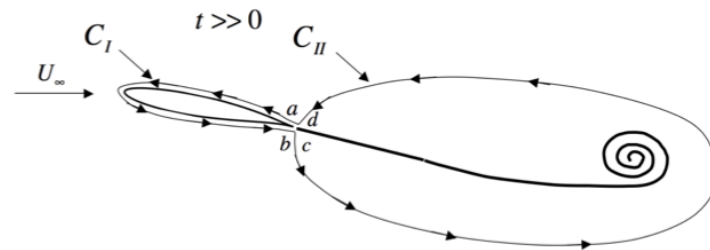
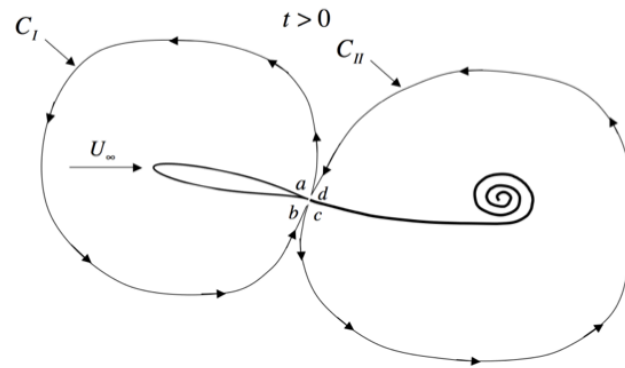
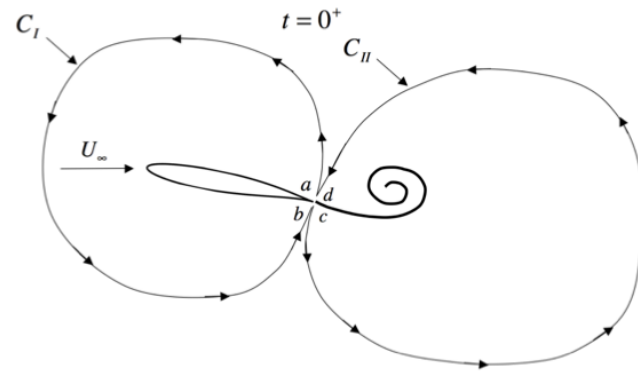
$$W = -\frac{i\Gamma}{2\pi} \text{Ln}(z) \quad \Phi = \frac{\Gamma}{2\pi} \theta \quad \Psi = -\frac{\Gamma}{2\pi} \text{Ln}(r) \quad (10.95)$$



The velocity field is directed in the counter-clockwise direction - circulation is positive.

For any contour  $C$  surrounding the origin

$$\int_A \Omega dA = \int_A \nabla \times \bar{U} dA = \oint_C \bar{U} \hat{c} dC = \int_0^{2\pi} \frac{\Gamma}{2\pi r} r d\theta = \Gamma \quad (10.96)$$



$$\int_a^b \mathbf{U} \cdot \hat{\mathbf{c}} dC + \int_c^d \mathbf{U} \cdot \hat{\mathbf{c}} dC = \oint_{C_1 + C_2} \nabla \Phi \cdot \hat{\mathbf{c}} dC = 0 \quad (11.2)$$

$$\Gamma_{Wing} = -\Gamma_{Vortex} \quad (11.3)$$



The downwash from the starting vortex reduces the effective angle of attack and rotates the normal force vector producing drag

$$L = F_N \cos(\alpha_i) = F_N \frac{U_\infty}{(U_\infty^2 + U_{yi}(0,0,t)^2)^{1/2}} \quad (11.10)$$

$$D_i = -F_N \sin(\alpha_i) = -F_N \frac{U_{yi}(0,0,t)}{(U_\infty^2 + U_{yi}(0,0,t)^2)^{1/2}} \cdot \quad (11.11)$$

$$F_N = -\rho U_R \Gamma_{Wing} \cdot \quad (11.12)$$

$$L = F_N \cos(\alpha_i) = -\rho U_\infty \Gamma_{Wing} \quad (11.13)$$

$$D_i = \rho U_{yi}(0,0,t) \Gamma_{Wing} \cdot \quad (11.14)$$

$$D_i = \rho \frac{\Gamma^2}{2\pi U_\infty t} \cdot \quad (11.15)$$

$$C_L = \frac{L}{\frac{1}{2} \rho U_\infty^2 C} = a_0 (\alpha + \alpha_i) \quad (11.16)$$

Solve for the circulation

$$-\rho U_\infty \Gamma_{Wing} = a_0 \frac{1}{2} \rho U_\infty^2 C \left( \alpha + \frac{\Gamma_{Wing}}{2\pi U_\infty^2 t} \right) \cdot \quad (11.17)$$

Onset of circulation

$$\frac{-2\Gamma_{Wing}(t)}{U_\infty C} = \left( \frac{\frac{4\pi U_\infty t}{a_0 C}}{\frac{4\pi U_\infty t}{a_0 C} + 1} \right) a_0 \alpha = C_L(t) \quad (11.18)$$

Onset of lift

$$C_L(t) = \left( \frac{\frac{4\pi U_\infty t}{a_0 C}}{\frac{4\pi U_\infty t}{a_0 C} + 1} \right) a_0 \alpha \quad (11.19)$$

Growth and decay of drag

$$C_{D_i}(t) = \left( \frac{\frac{4\pi U_\infty t}{a_0 C}}{\left( \frac{4\pi U_\infty t}{a_0 C} + 1 \right)^2} \right) a_0 \alpha^2$$

Time constant

$$\tau_{Starting\ Airfoil} = \frac{a_0 C}{4\pi U_\infty} \quad (11.20)$$

According to classical theory

$$a_0 = 2\pi$$



$$\frac{-2\Gamma_{\text{Wing}}(t)}{a_0 U_\infty C \alpha} = \frac{C_L}{a_0 \alpha} = \left( \frac{t / \tau_{\text{Starting Airfoil}}}{t / \tau_{\text{Starting Airfoil}} + 1} \right), \quad \frac{C_{D_i}}{a_0 \alpha^2} = \left( \frac{t / \tau_{\text{Starting Airfoil}}}{(t / \tau_{\text{Starting Airfoil}} + 1)^2} \right). \quad (11.21)$$

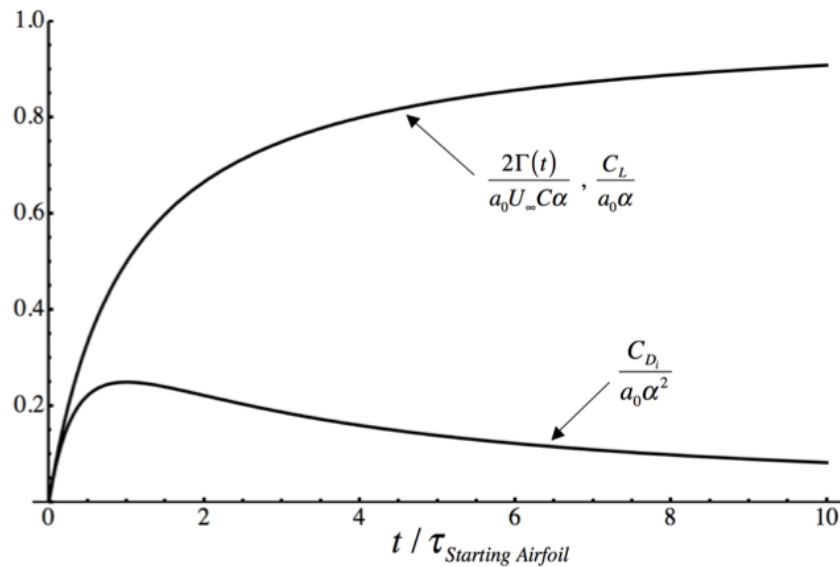
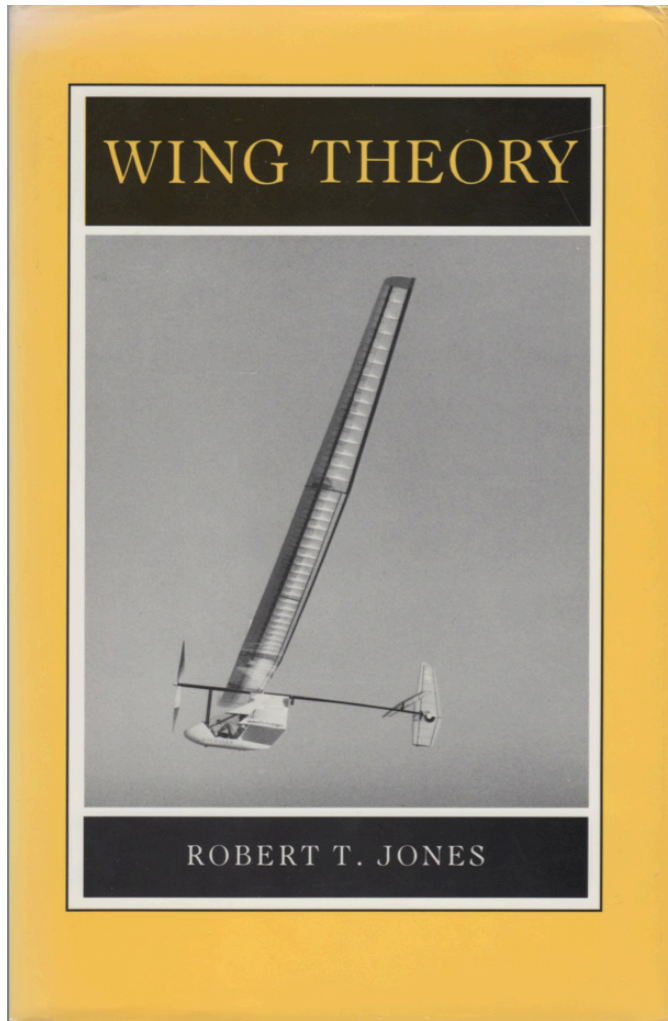
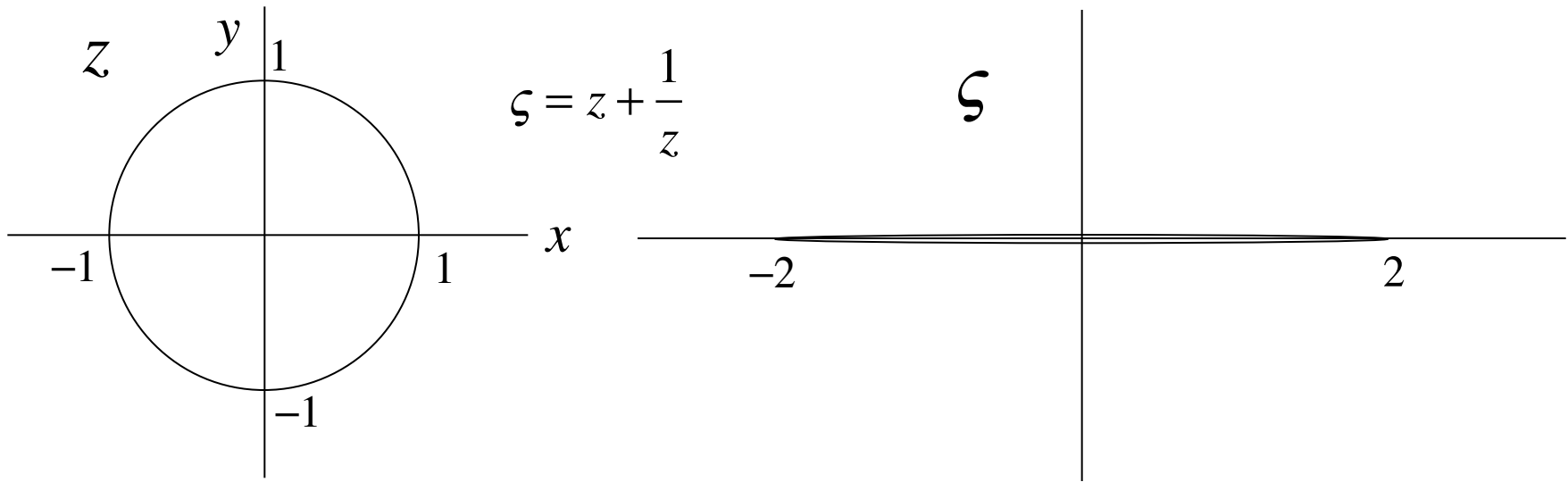


*Figure 11.4 Onset of circulation and lift, growth and decay of induced drag on an impulsively started airfoil.*

## The Joukowski airfoil - from *Wing Theory* by R. T. Jones chapter 3



# The Joukowski transformation



The Joukowski transformation maps a circle of unit radius centered at the origin to the upper and lower surface of a horizontal line joining -2 and +2. For example

$$z = re^{i\theta} = 1 + i0$$

$$\zeta = z + \frac{1}{z} = 1 + 1 = 2$$

$$z = re^{i\theta} = -1 + i0$$

$$\zeta = z + \frac{1}{z} = -1 - 1 = -2$$

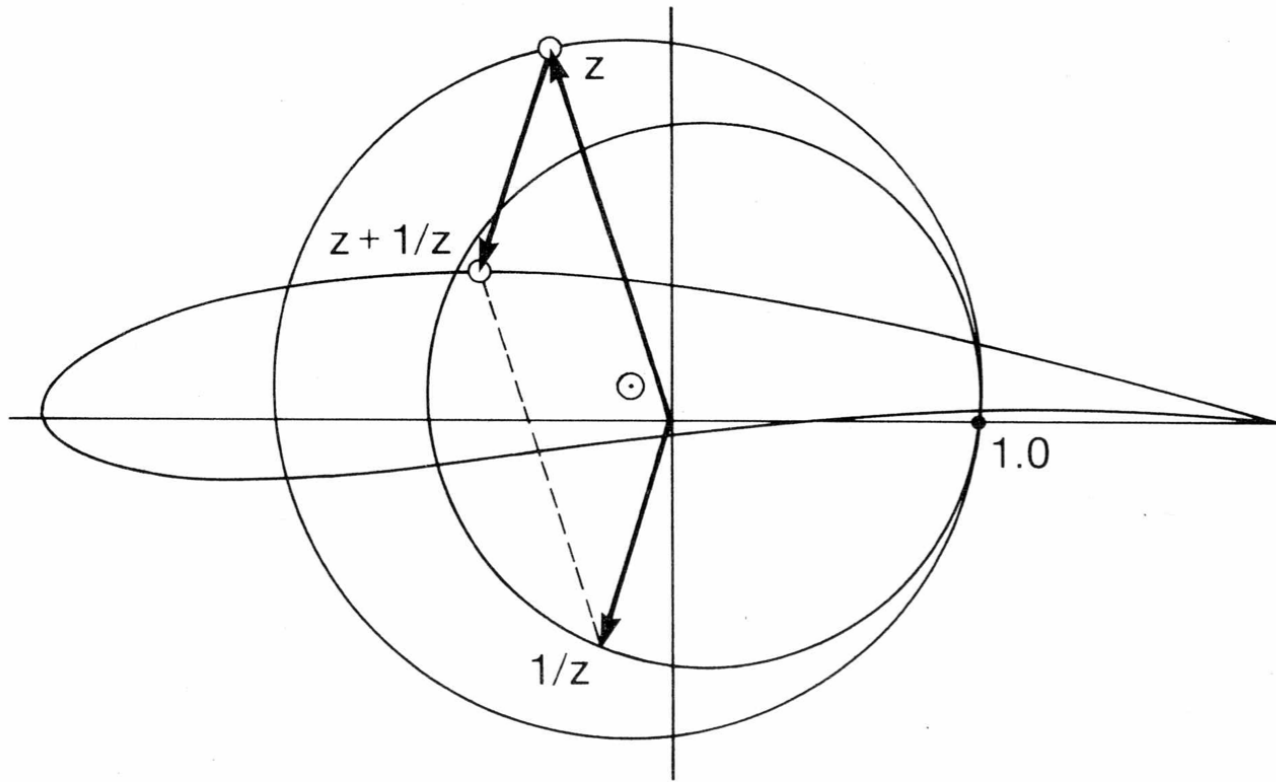
$$z = re^{i\theta} = (1 + \varepsilon)e^{i\pi/2} = 0 + i(1 + \varepsilon)$$

$$\zeta = z + \frac{1}{z} = i(1 + \varepsilon) - \frac{i}{1 + \varepsilon} = i \left( \frac{(1 + \varepsilon)^2 - 1}{1 + \varepsilon} \right) \doteq i2\varepsilon$$

$$z = re^{i\theta} = (1 + \varepsilon)e^{-i\pi/2} = 0 - i(1 + \varepsilon)$$

$$\zeta = z + \frac{1}{z} = -i(1 + \varepsilon) + \frac{i}{1 + \varepsilon} = -i \left( \frac{(1 + \varepsilon)^2 - 1}{1 + \varepsilon} \right) \doteq -i2\varepsilon$$

The Joukowski transformation maps a circle of greater than unit radius with the origin offset from (0,0) to the upper and lower surface of a wing with its trailing edge at +2.



### 3.2. Transformation of circle to airfoil.

R.T. Jones describes a sequence of transformations.

1) Translate the origin and select the trailing edge - this determines the radius of the circle.

$$z_2 = z_1 + z_{2c} \quad \text{where} \quad z_{2c} = x_{2c} + iy_{2c} \quad R = \left( (x_{2c} - x_{2t})^2 + (y_{2c} - y_{2t})^2 \right)^{1/2}$$

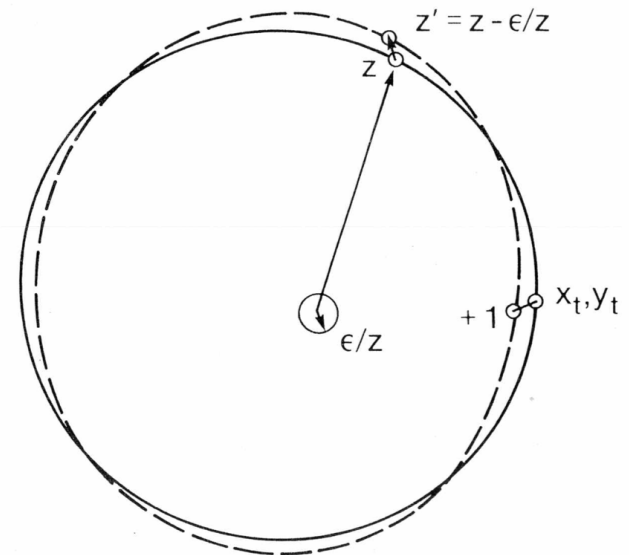
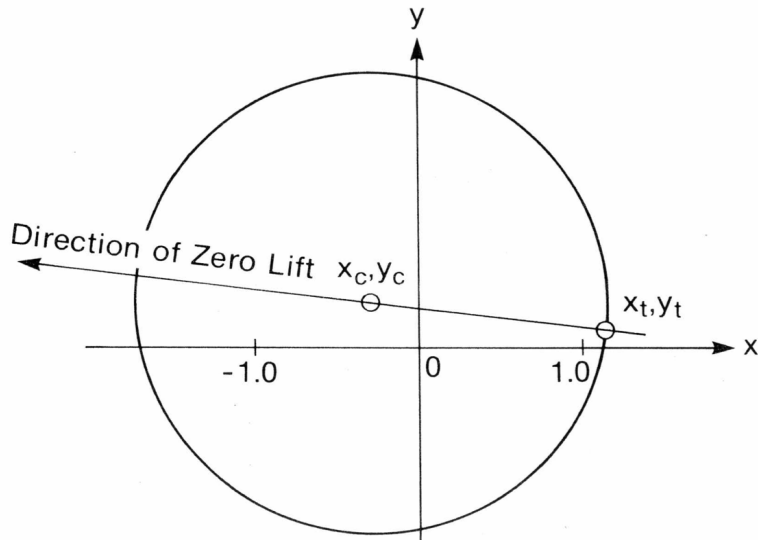
2) Map the circle to an oval with the trailing edge at (1,0).

$$z_3 = z_2 - \frac{\epsilon}{z_2 - \Delta}$$

Choose the real and imaginary parts of epsilon so that

$$z_{3t} = z_{2t} - \frac{\epsilon_r + i\epsilon_i}{z_{2t} - \Delta} = 1 + i(0)$$

$$\begin{aligned} \epsilon_r &= (x_{2TE} - 1)(x_{2TE} - \Delta) - y_{2TE}^2 \\ \epsilon_i &= y_{2TE} (2x_{2TE} - 1 - \Delta) \end{aligned}$$

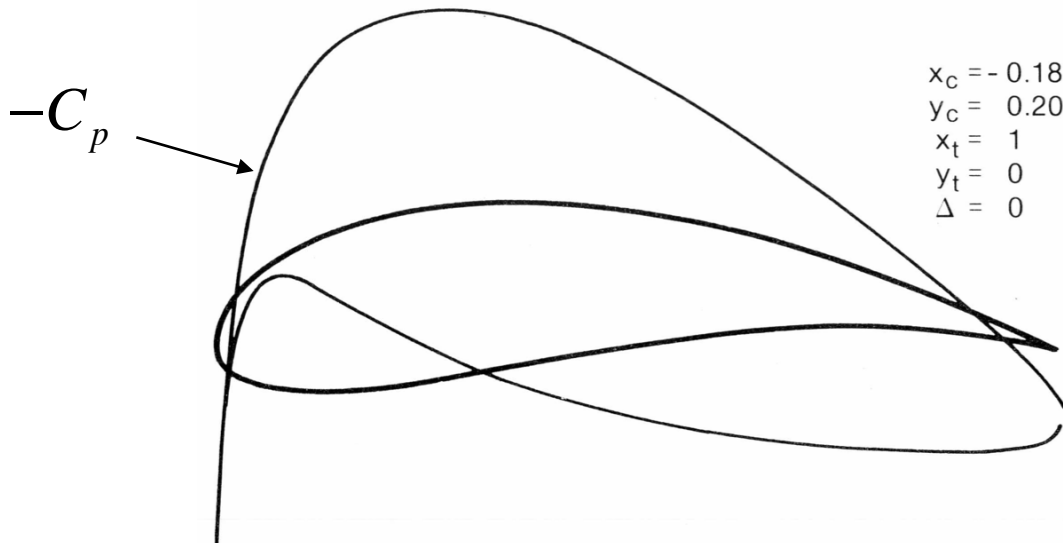


3) Map the oval to an airfoil with the trailing edge at (2,0).

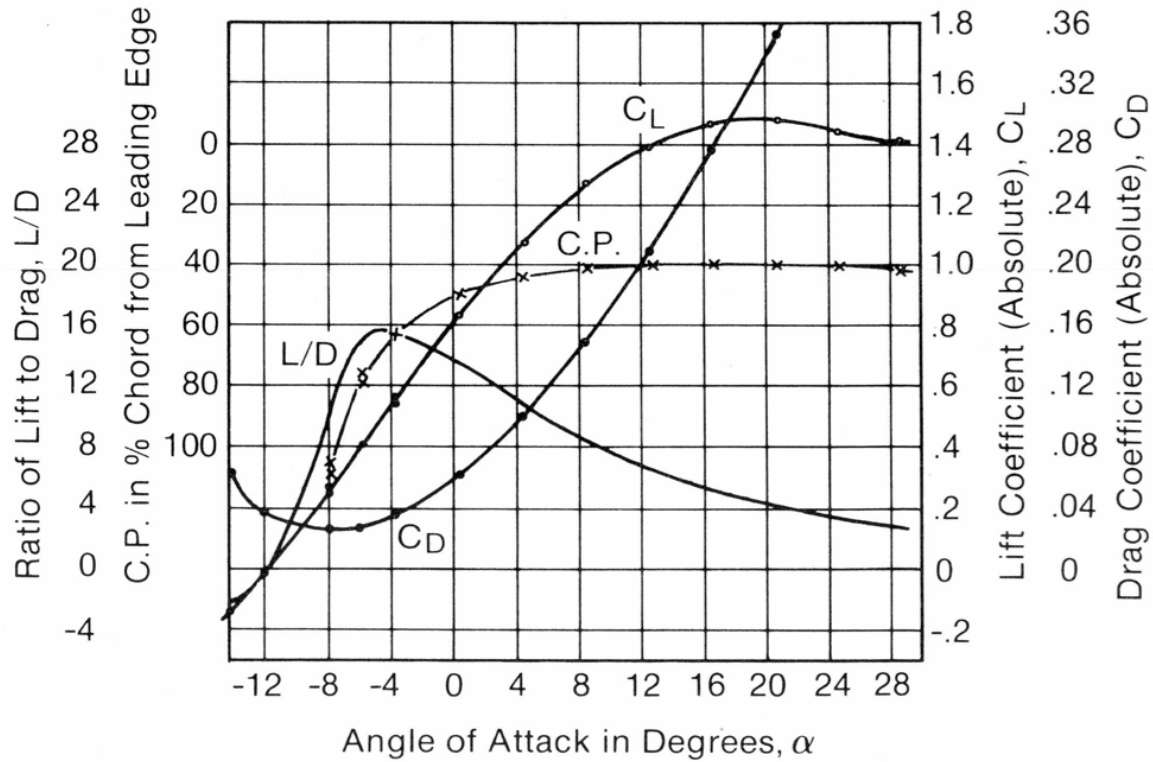
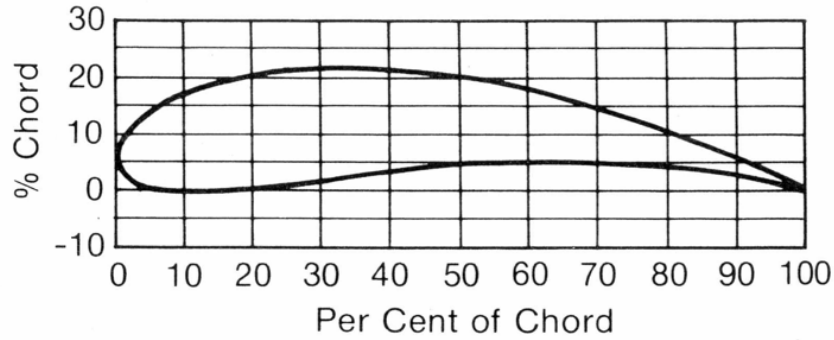
$$z = z_3 + \frac{1}{z_3}$$

Overall mapping

$$z = \left( (z_1 + z_{2c}) - \frac{\epsilon_r + i\epsilon_i}{(z_1 + z_{2c}) - \Delta} \right) + \frac{1}{\left( (z_1 + z_{2c}) - \frac{\epsilon_r + i\epsilon_i}{z_1 + z_{2c} - \Delta} \right)}$$



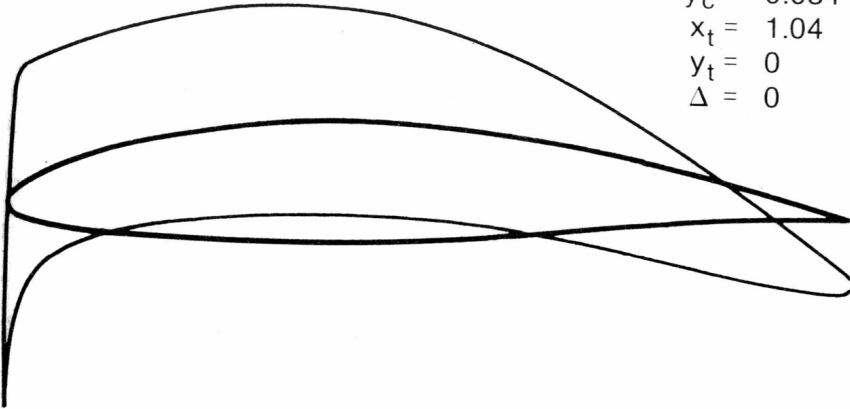
3.5. NACA 101 (Joukowski).



3.6. Joukowski airfoil tested in NACA variable density wind tunnel.

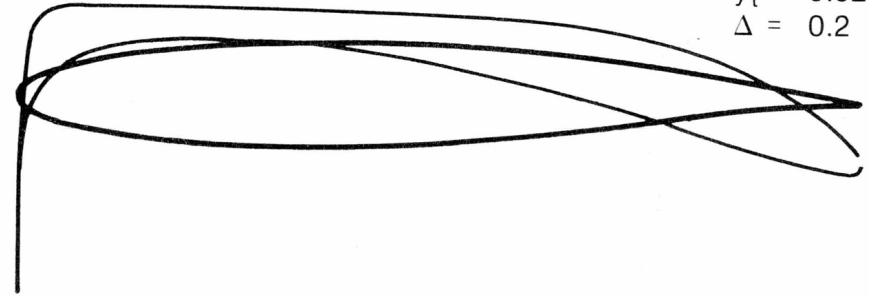
## Some examples with pressure distributions

$$\begin{aligned}
 x_c &= -0.0707 \\
 y_c &= 0.084 \\
 x_t &= 1.04 \\
 y_t &= 0 \\
 \Delta &= 0
 \end{aligned}$$



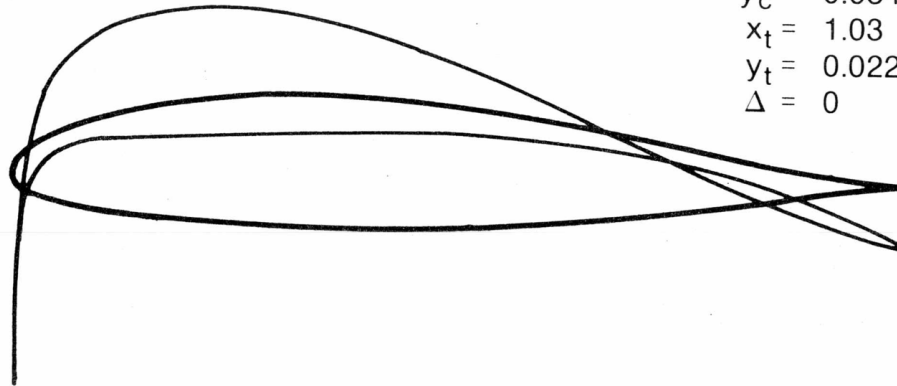
71 3.9. Laminar flow airfoil.

$$\begin{aligned}
 x_c &= -0.07 \\
 y_c &= 0.02 \\
 x_t &= 1.03 \\
 y_t &= -0.02 \\
 \Delta &= 0.2
 \end{aligned}$$



3.10. Minimum velocity airfoil.

$$\begin{aligned}
 x_c &= -0.094 \\
 y_c &= 0.034 \\
 x_t &= 1.03 \\
 y_t &= 0.022 \\
 \Delta &= 0
 \end{aligned}$$



3.11. Reflex airfoil.



AA200A Homework 6 2014 -2015

Due Tuesday May 19, 2015

Read: Chapter 11

Recommended Reading: Chapter 3 in *Wing Theory* by R. T. Jones

**Problem 1** – Reproduce the results in section 11.2 for the flow around a Joukowski airfoil. Using that airfoil or, if wish a Joukowski airfoil based on your own choice of parameters, determine the lift coefficient for a range of angles of attack.

Select several angles of attack for more detailed study in the following two problems.

**Problem 2** – Determine the thickness function and camber function for the Joukowski wing you generated in problem 1. Use these functions to produce the thin airfoil approximation to this wing. Determine the thin airfoil pressure coefficient about the wing and compare to the pressure coefficient from Joukowski theory. Determine the lift and moment coefficients of the wing based on thin airfoil theory.

**Problem 3** – Now that you have defined a wing geometry with its pressure distribution determine the boundary layer characteristics on the wing.

1) Assume a laminar boundary layer and use Thwaites' method to determine the boundary layer characteristics on the upper and lower surfaces up to separation.

2) Assume a turbulent boundary layer and use Head's method to determine the boundary layer characteristics on the upper and lower surfaces up to separation. Determine the drag coefficient of the wing. Plot  $L/D$  versus angle of attack. You may wish to use a Thwaites calculation for laminar flow very near the wing leading edge to provide initial conditions for a Head's calculation over the rest of the wing.

## 11.2 The Joukowski airfoil - Class notes

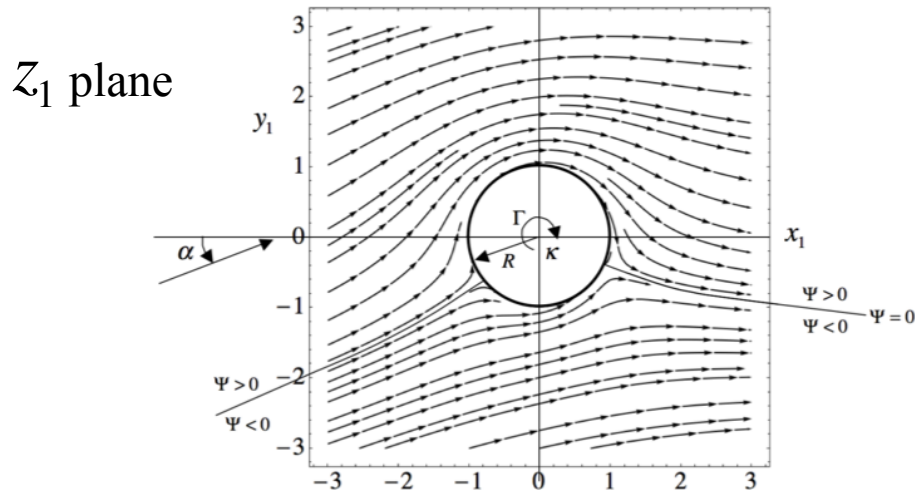
$$W(z_1) = U_\infty z_1 e^{-i\alpha} + \frac{\kappa}{2\pi} \left( \frac{1}{z_1} \right) + \frac{i\Gamma}{2\pi} \text{Ln}(z_1)$$

$$\Phi(x_1, y_1) = U_\infty (x_1 \cos(\alpha) + y_1 \sin(\alpha)) + \frac{\kappa}{2\pi} \left( \frac{x_1}{x_1^2 + y_1^2} \right) - \frac{\Gamma}{2\pi} \text{ArcTan}(y_1 / x_1) \quad (11.31)$$

$$\Psi = U_\infty (y_1 \cos(\alpha) - x_1 \sin(\alpha)) + \frac{\kappa}{2\pi} \left( \frac{y_1}{x_1^2 + y_1^2} \right) + \frac{\Gamma}{2\pi} \text{Ln}((x_1^2 + y_1^2)^{1/2})$$

$$R = \sqrt{\frac{\kappa}{2\pi R U_\infty}} \quad (11.32) \quad \text{Note correction!}$$

The flow is shown below for  $\gamma = 1$ ,  $R = 1$  and  $\alpha = \pi / 18$ .



Circulation in the clockwise direction has been taken to be positive. This is commonly done in aerodynamics (eg. RT Jones)

Figure 11.6 Flow at angle of attack  $\alpha$  past a circular cylinder with lift.

## Non-dimensionalize the potentials and circulation

$$w(z_1) = \left(\frac{z_1}{R}\right) e^{-i\alpha} + \left(\frac{R}{z_1}\right) + i\gamma \text{Ln}\left(\frac{z_1}{R}\right)$$

$$\phi(x_1, y_1) = \left(\frac{x_1}{R}\right) \text{Cos}(\alpha) + \left(\frac{y_1}{R}\right) \text{Sin}(\alpha) + \frac{R \text{Cos}(\theta_1)}{r_1} - \gamma \theta_1 \quad (11.33)$$

$$\psi(x_1, y_1) = y_1 \text{Cos}(\alpha) - x_1 \text{Sin}(\alpha) - \frac{R \text{Sin}(\theta_1)}{r_1} + \gamma \text{Ln}\left(\frac{r_1}{R}\right)$$

$$w = \frac{W}{U_\infty R} \quad \phi = \frac{\Phi}{U_\infty R} \quad \psi = \frac{\Psi}{U_\infty R} \quad (11.34)$$

$$\gamma = \frac{\Gamma}{2\pi R U_\infty} \quad (11.35)$$

In cylindrical coordinates

$$\begin{aligned}\phi &= \frac{r_1}{R} \cos(\alpha) \cos(\theta_1) + \frac{r_1}{R} \sin(\alpha) \sin(\theta_1) + \frac{R}{r_1} \cos(\theta_1) - \gamma \theta_1 \\ \psi &= \frac{r_1}{R} \cos(\alpha) \sin(\theta_1) - \frac{r_1}{R} \sin(\alpha) \cos(\theta_1) - \frac{R}{r_1} \sin(\theta_1) + \gamma \ln\left(\frac{r_1}{R}\right)\end{aligned}\quad (11.36)$$

Complex velocity

$$\frac{dw(z_1)}{dz_1} = \frac{e^{-i\alpha}}{R} - \left(\frac{R}{z_1^2}\right) + i \frac{\gamma}{z_1} \quad (11.37)$$

Velocity components

$$\begin{aligned}U_{r_1} &= \frac{1}{R} \cos(\alpha) \cos(\theta_1) + \frac{1}{R} \sin(\alpha) \sin(\theta_1) - \frac{R}{r_1^2} \cos(\theta_1) \\ U_{\theta_1} &= -\frac{1}{R} \cos(\alpha) \sin(\theta_1) + \frac{1}{R} \sin(\alpha) \cos(\theta_1) - \frac{R}{r_1^2} \sin(\theta_1) - \frac{\gamma}{r_1}\end{aligned}\quad (11.38)$$

Tangential velocity at the cylinder surface

$$U_{\theta_1} \Big|_{r_1=R} = \frac{1}{R} \left( -\text{Cos}(\alpha) \text{Sin}(\theta_1) + \text{Sin}(\alpha) \text{Cos}(\theta_1) - \text{Sin}(\theta_1) - \gamma \right) . \quad (11.39)$$

Stagnation points occur where the tangential velocity is zero

$$\text{Sin}(\alpha) \text{Cos}(\theta_{10}) = \text{Cos}(\alpha) \text{Sin}(\theta_{10}) + \text{Sin}(\theta_{10}) + \gamma . \quad (11.40)$$

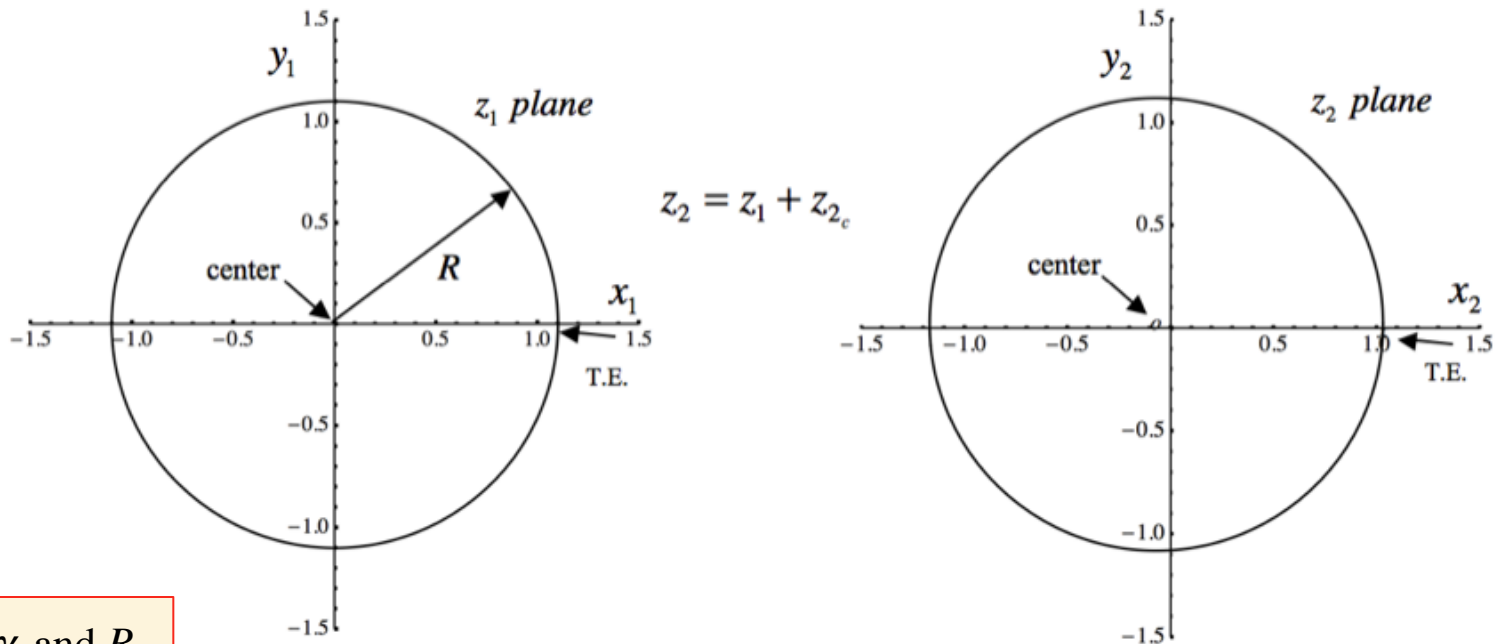
Stagnation point angles

$$\text{Sin}(\theta_{10}) = -\frac{\gamma}{2} \pm \frac{\text{Sin}(\alpha)}{2(1 + \text{Cos}(\alpha))} \sqrt{2(1 + \text{Cos}(\alpha)) - \gamma^2} . \quad (11.41)$$

Step 1 – Translate the circle in the  $z_1$  plane to a circle in the  $z_2$  plane with its origin shifted from  $(0,0)$ . The mapping is

$$z_2 = z_1 + z_{2c} \quad \text{where} \quad z_{2c} = x_{2c} + iy_{2c} \quad . \quad (11.42)$$

Specify the coordinates of the center of the circle in the  $z_2$  plane  $(x_{2c}, y_{2c})$ . In addition specify the coordinates of the trailing edge  $(x_{2t}, y_{2t})$  in the  $z_2$  plane. Now the radius of the circle in the  $z_1$  plane is determined.



Note that  $\gamma$  and  $R$  determine  $C_L$   
 $C_L = \pi\gamma R$

$$R = \left( (x_{2c} - x_{2t})^2 + (y_{2c} - y_{2t})^2 \right)^{1/2} \quad (11.43)$$

Step 2 – Map the circle in  $z_2$  to an oval in the  $z_3$  plane passing through the point  $(x_3, y_3) = (1, 0)$ . The mapping is

$$z_3 = z_2 - \frac{\varepsilon}{z_2 - \Delta} \quad (11.44)$$

where  $\varepsilon$  is complex and  $\Delta$  is real. We require that the coordinates of the trailing edge  $z_{2t} = x_{2t} + iy_{2t}$  satisfy

$$z_{3t} = z_{2t} - \frac{\varepsilon_r + i\varepsilon_i}{z_{2t} - \Delta} = 1 + i(0) \quad (11.45)$$

Solve (11.45) for  $(\varepsilon_r, \varepsilon_i)$  using  $x_{3t} = 1$  and  $y_{3t} = 0$ .

$$\begin{aligned} \varepsilon_r &= (x_{2_{TE}} - 1)(x_{2_{TE}} - \Delta) - y_{2_{TE}}^2 \\ \varepsilon_i &= y_{2_{TE}}(2x_{2_{TE}} - 1 - \Delta) \end{aligned} \quad (11.46)$$

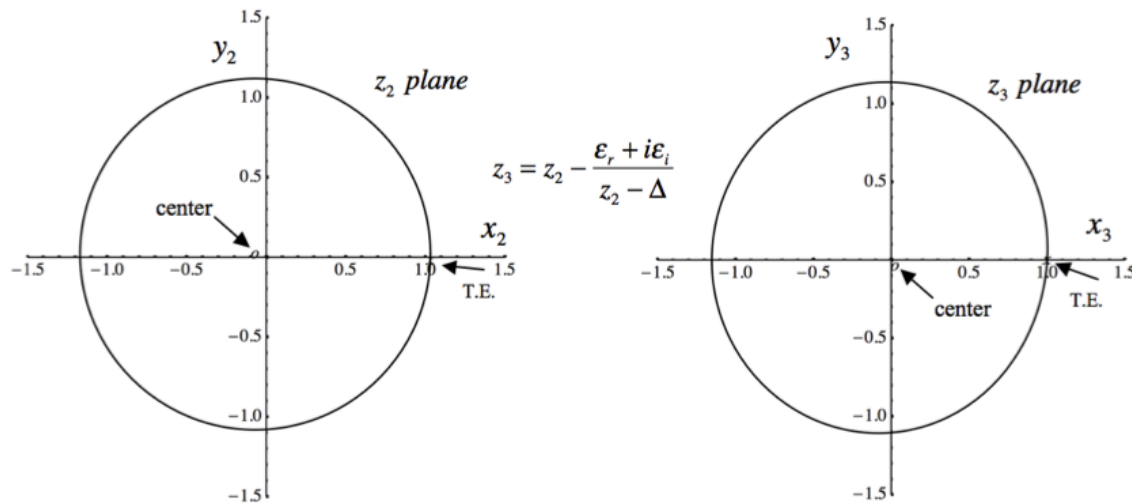


Figure 11.8 Mapping from  $z_2$  to  $z_3$ .

Step 3 – Map the oval to an airfoil using the Joukowski transformation.

$$z = z_3 + \frac{1}{z_3} \quad (11.47)$$

The overall transformation from the circle to airfoil coordinates is

$$z = \left( (z_1 + z_{2c}) - \frac{\epsilon_r + i\epsilon_i}{(z_1 + z_{2c}) - \Delta} \right) + \frac{1}{\left( (z_1 + z_{2c}) - \frac{\epsilon_r + i\epsilon_i}{z_1 + z_{2c} - \Delta} \right)}. \quad (11.48)$$

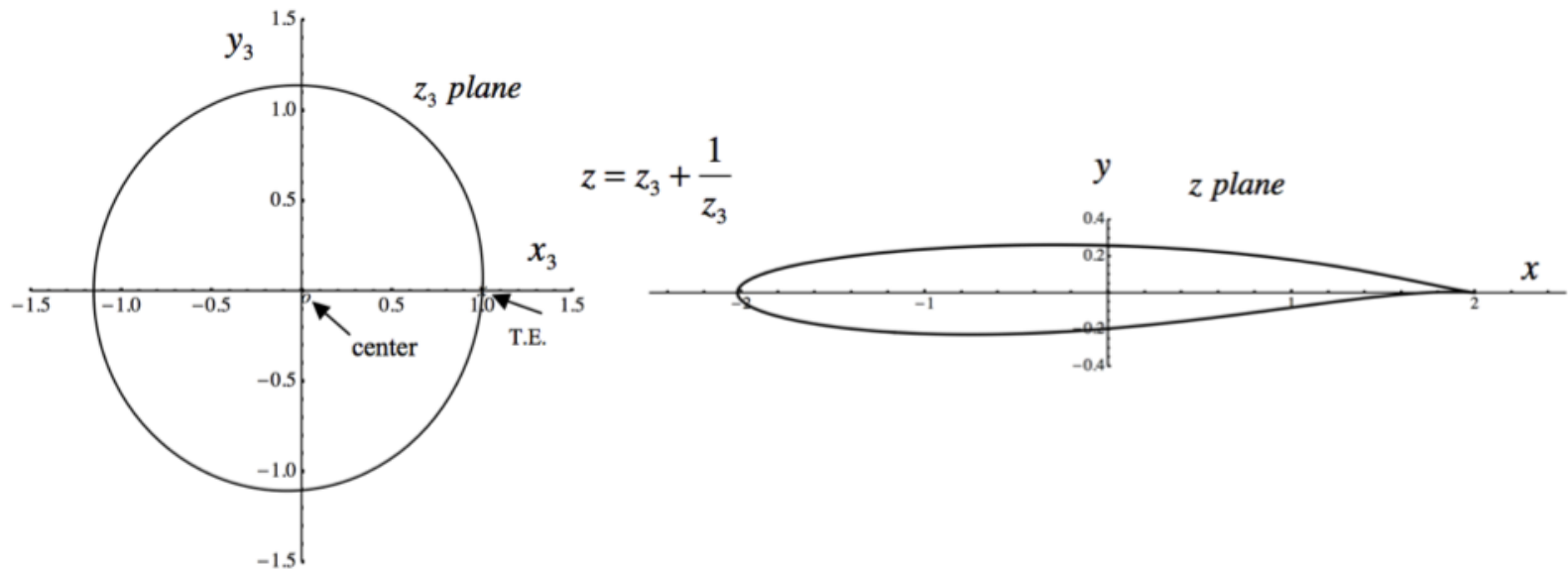


Figure 11.9 Mapping from  $z_3$  to  $z$ .



**Example – Joukowski airfoil.**

Choose the following values.

$$\alpha = \pi / 9 \quad x_{2c} = -0.07 \quad y_{2c} = 0.02 \quad x_{2TE} = 1.03 \quad y_{2TE} = -0.02 \quad \Delta = 0.2 \quad (11.49)$$

The coordinates of the center of the circle  $(x_{2c}, y_{2c})$  and the trailing edge  $(x_{2t}, y_{2t})$  in the  $z_2$  plane determine the radius of the circle in the  $z_1$  plane.

$$R = \left( (x_{2c} - x_{2t})^2 + (y_{2c} - y_{2t})^2 \right)^{1/2} = \left( (0.07 - 1.03)^2 + (0.02 + 0.02)^2 \right)^{1/2} = 1.10073 \quad (11.50)$$

The location of the trailing edge in the  $z_1$  plane is determined using (11.42).

$$\begin{aligned} z_{1TE} &= z_{2TE} - z_{2c} = 1.10 - 0.04i \\ \theta_{10TE} &= \text{ArcTan} \left( \frac{-0.04}{1.10} \right) = -0.03635 \quad . \end{aligned} \quad (11.51)$$

Now apply the Kutta condition. The dimensionless circulation (11.35) is chosen to insure that the rear stagnation point on the circle in the  $z_1$  plane depicted in Figure 11.6 is located at the point (11.51) designated as the trailing edge. In other words, when we choose the parameters (11.49) the radius of the circle in the  $z_1$  plane, the angle of the trailing edge and the value of  $\gamma$  in (11.41) that gives the angle calculated in (11.51) as the root are all determined. The circulation is determined to be

$$\gamma = \text{Sin}(\alpha) \text{Cos}(\theta_{10TE}) - \text{Cos}(\alpha) \text{Sin}(\theta_{10TE}) - \text{Sin}(\theta_{10TE}) = 0.412282 \quad . \quad (11.52)$$

Note that  $\Delta$  does not affect  $\gamma$

The angle of the forward stagnation point in the  $z_1$  plane is determined from (11.41). The roots are

$$\theta_{10} = \text{ArcSin} \left( -\frac{\gamma}{2} \pm \frac{\text{Sin}(\alpha)}{2(1 + \text{Cos}(\alpha))} \sqrt{2(1 + \text{Cos}(\alpha)) - \gamma^2} \right) = (-2.7562, -0.03635) \quad (11.53)$$

The position of the nose stagnation point in the  $z_1$  plane is

$$z_{1nose} = -1.01998 - 0.41381i \quad (11.54)$$

and the position in the  $z_2$  plane is

$$z_{2nose} = -1.08998 - 0.39381i . \quad (11.55)$$

$$\begin{aligned} \epsilon_r &= (x_{2_{TE}} - 1)(x_{2_{TE}} - \Delta) - y_{2_{TE}}^2 = (1.03 - 1)(1.03 - 0.2) - (0.02)^2 = 0.0245 \\ \epsilon_i &= y_{2_{TE}} (2x_{2_{TE}} - 1 - \Delta) = -0.02(2(1.03) - 1 - 0.2 - 0.02) = -0.0172 \end{aligned} \quad (11.56)$$

The airfoil coordinates are

$$x + iy = \left( \frac{R \text{Cos}(\theta) + iR \text{Sin}(\theta) + x_{2c} + iy_{2c} - \frac{\epsilon_r + i\epsilon_i}{R \text{Cos}(\theta) + iR \text{Sin}(\theta) + x_{2c} + iy_{2c} - \Delta}}{1} \right) + \frac{1}{\left( R \text{Cos}(\theta) + iR \text{Sin}(\theta) + x_{2c} + iy_{2c} - \frac{\epsilon_r + i\epsilon_i}{R \text{Cos}(\theta) + iR \text{Sin}(\theta) + x_{2c} + iy_{2c} - \Delta} \right)} \quad (11.57)$$

## Complex velocity

$$\frac{dW}{dz} = \frac{dW}{dz_1} \frac{dz_1}{dz_2} \frac{dz_2}{dz_3} \frac{dz_3}{dz} . \quad (11.58)$$

$$\frac{dz_1}{dz_2} = 1$$

$$\frac{dz_2}{dz_3} = \frac{1}{\left(\frac{dz_3}{dz_2}\right)} = \frac{1}{\left(1 + \frac{\varepsilon}{(z_2 - \Delta)^2}\right)} = \frac{(z_2 - \Delta)^2}{(z_2 - \Delta)^2 + \varepsilon} . \quad (11.59)$$

$$\frac{dz_3}{dz} = \frac{1}{\left(\frac{dz}{dz_3}\right)} = \frac{z_3^2}{z_3^2 - 1}$$

$$U_z = U_{z_1} \left( \frac{(z_2 - \Delta)^2}{(z_2 - \Delta)^2 + \varepsilon} \right) \frac{z_3^2}{z_3^2 - 1} \quad (11.60)$$

$$\frac{dw(z_1)}{dz_1} = \frac{e^{-i\alpha}}{R} - \left( \frac{R}{z_1^2} \right) + i \frac{\gamma}{z_1} . \quad (11.61)$$

Zero velocities occur at:

i) The stagnation points in  $z_1$

ii)  $z_2 = \Delta$ ,  $z_3 = \infty$ ,  $z = \infty$

iii)  $z_3 = 0$ ,  $z = \infty$ .

Infinite velocities occur at  $z_1 = 0$  and:

i)  $z_3 = 1$ ,  $z = z_3 + 1 / z_3 = 2$ . The infinity multiplies the zero at the stagnation point to produce a finite velocity at the trailing edge.

ii)  $z_3 = 1$ ,  $z = -2$ . This point lies inside the airfoil.

iii) The point

$$\begin{aligned} (z_2 - \Delta)^2 + \varepsilon = 0 &\Rightarrow z_2 = \Delta \pm (-\varepsilon)^{1/2} \\ z_3 = \Delta \pm 2(-\varepsilon)^{1/2} & \end{aligned} \quad (11.62)$$

The singularity (11.62) transforms to

$$z_{Singularity} = \Delta + 2(-\varepsilon)^{1/2} + \frac{1}{\Delta + 2(-\varepsilon)^{1/2}}, \Delta - 2(-\varepsilon)^{1/2} + \frac{1}{\Delta - 2(-\varepsilon)^{1/2}} . \quad (11.63)$$

## Pressure distribution

$$z_{\text{Singularity}} = 1.81465 - 1.30801i, 0.906875 + 2.46541i \quad (11.64)$$

$$C_p = \frac{P - P_\infty}{\frac{1}{2}\rho U_\infty^2} = \left(1 - |U_z|^2\right) = 1 - (U_x^2 + U_y^2) \quad (11.65)$$

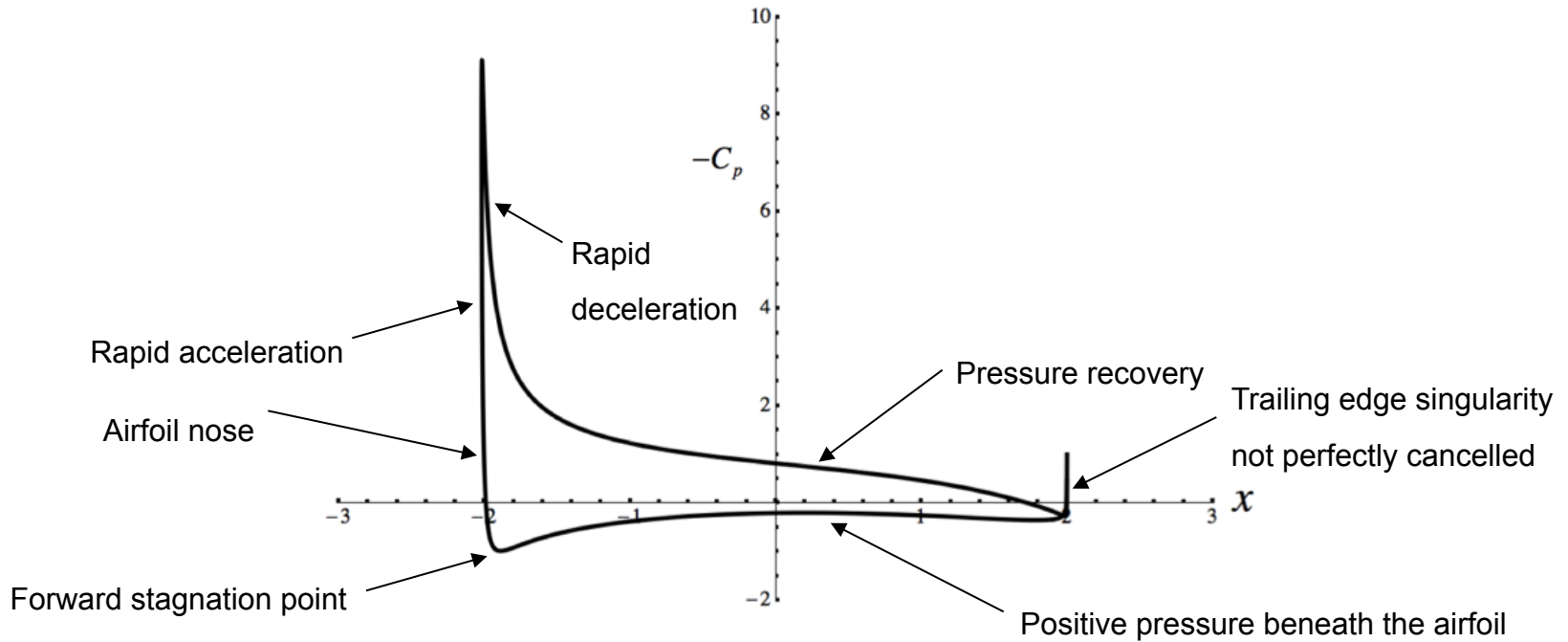
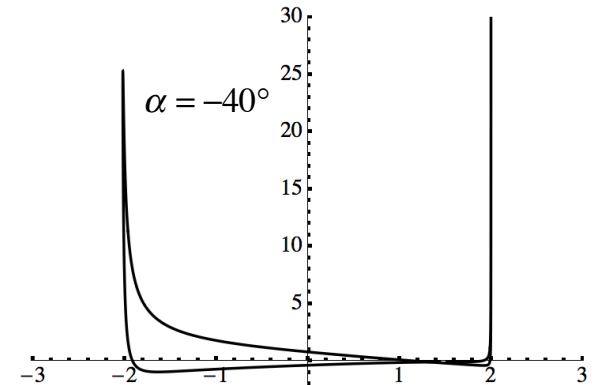
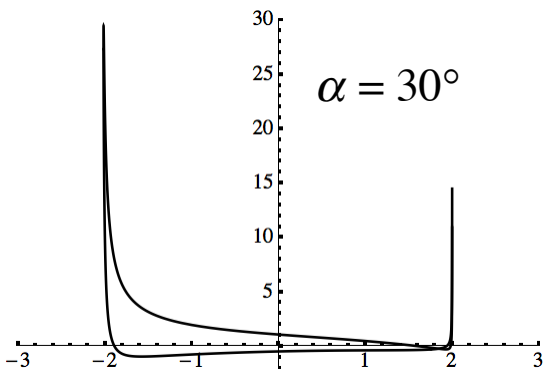
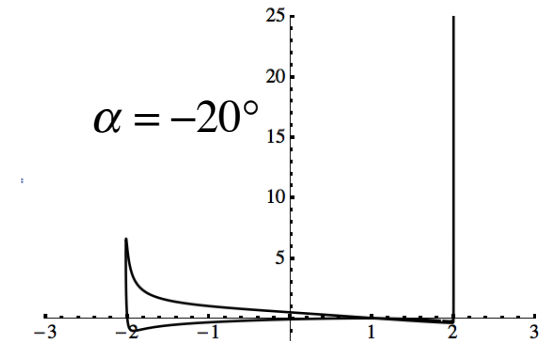
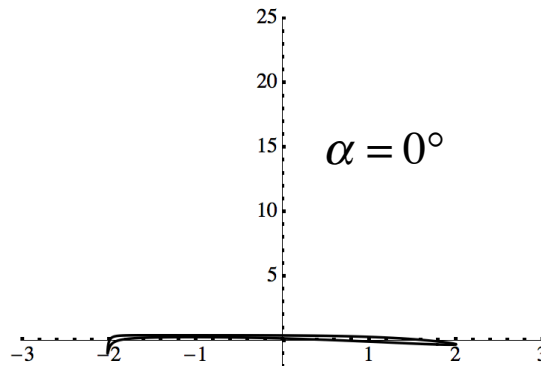
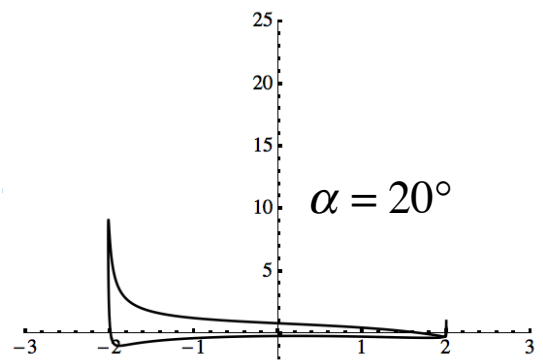
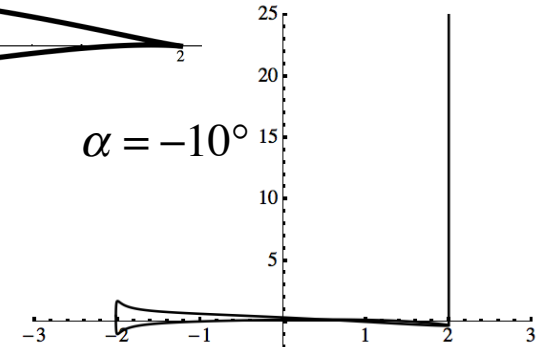
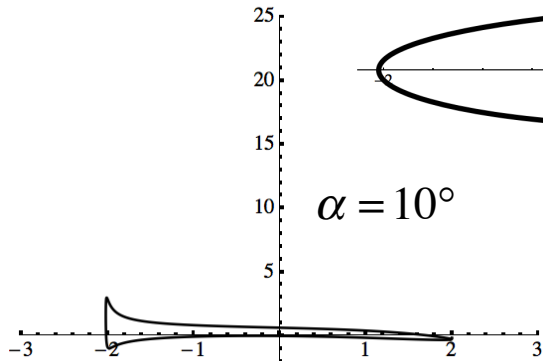
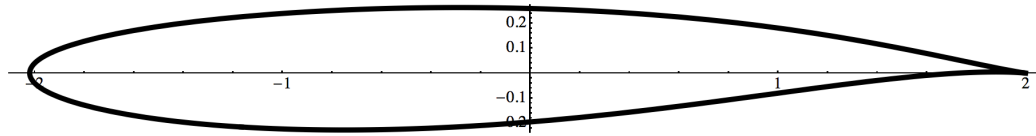


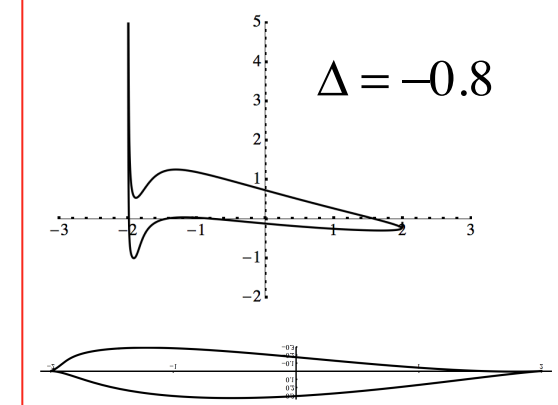
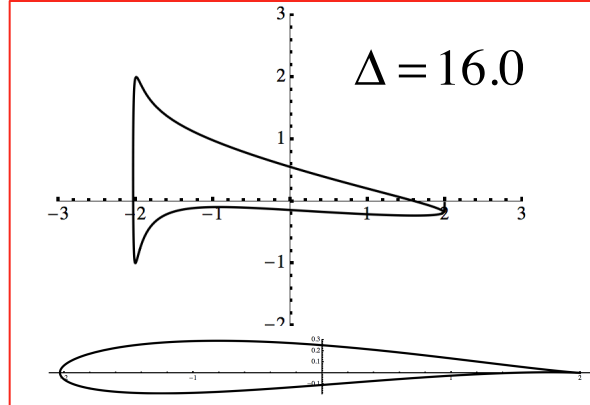
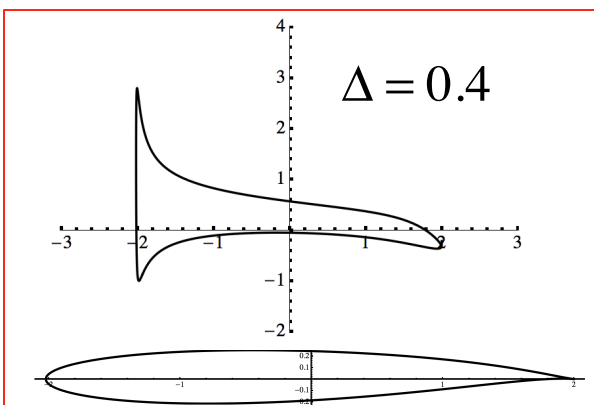
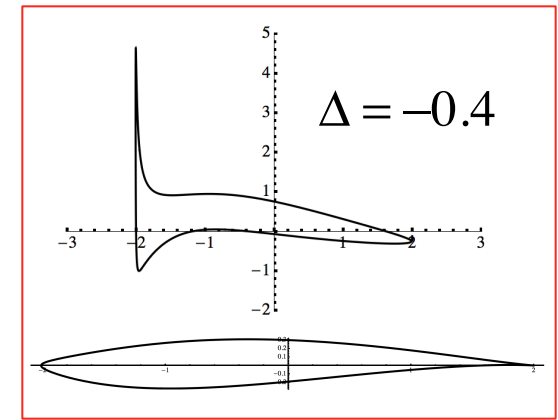
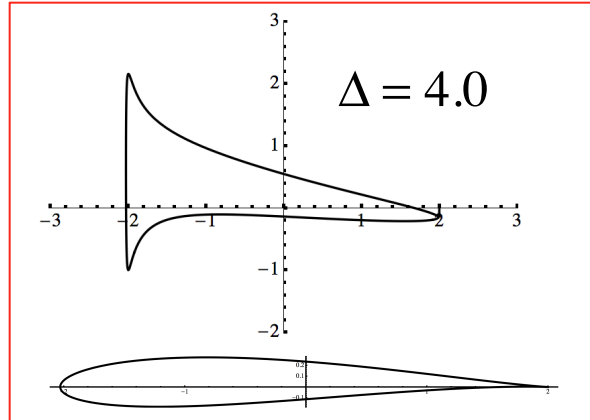
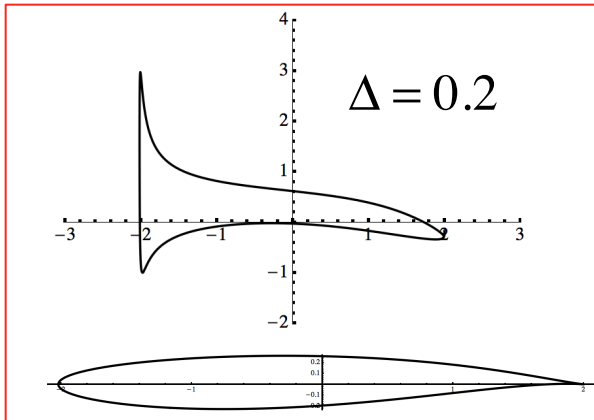
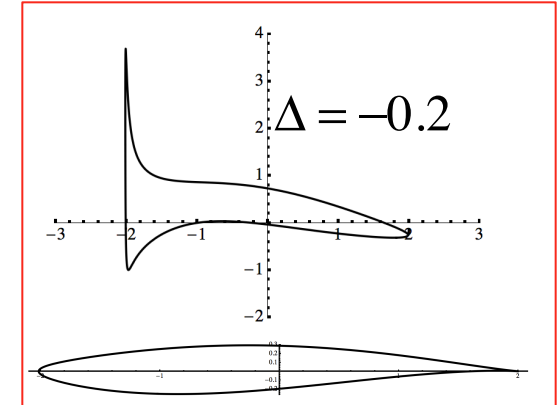
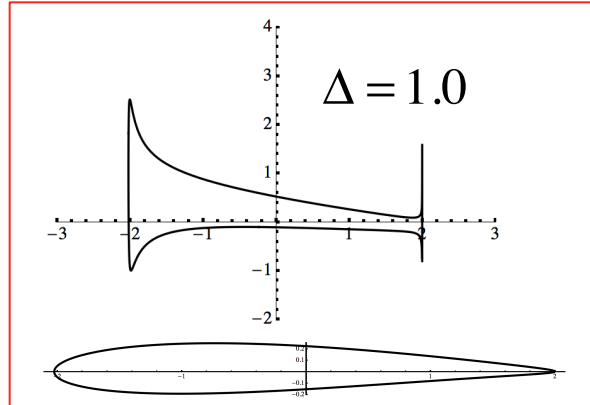
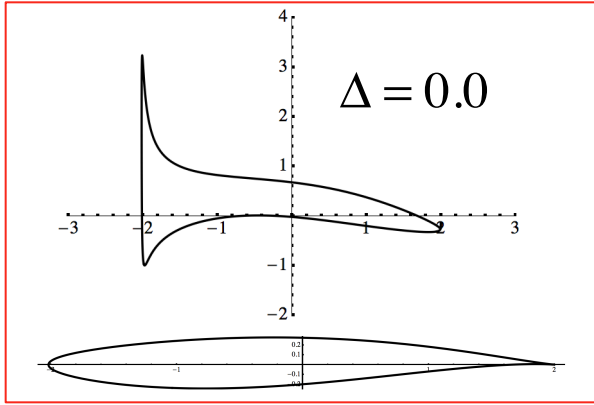
*Figure 11.10 pressure distributions on the example Joukowski airfoil at  $\alpha = \pi / 9$ .*

# $C_p$ at various angles of attack



# Effect of the parameter $\Delta$ on wing shape and $C_p$

$\alpha = 10^\circ$   
 $C_L = 0.85$



## 11.3 Thin airfoil theory

Thin airfoil theory allows us to design airfoils with nearly arbitrary characteristics. It works pretty well even on airfoils that are not all that thin.

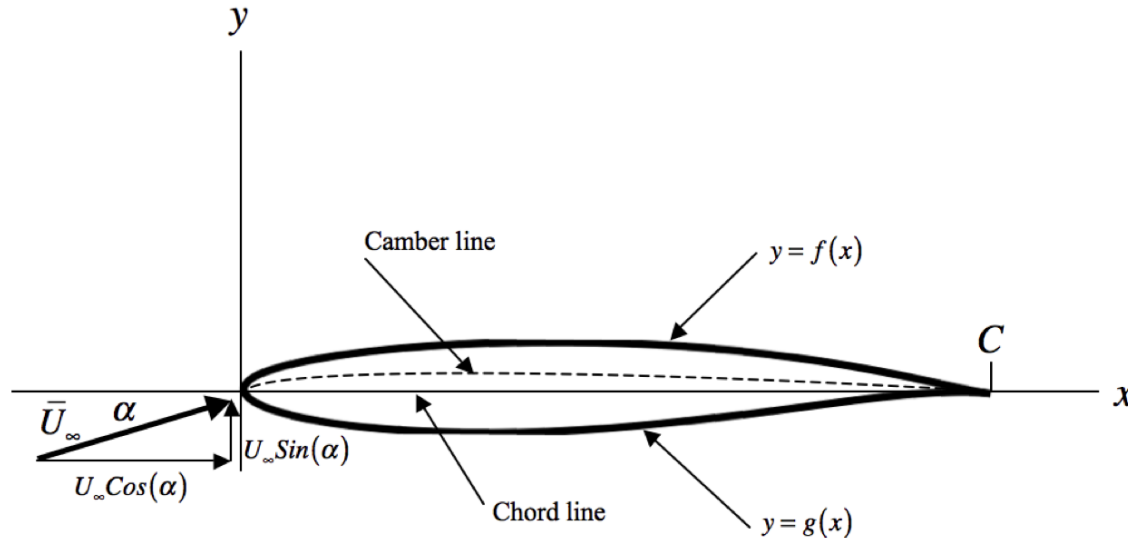


Figure 11.11 Two-dimensional airfoil at angle of attack  $\alpha$ .

$$\frac{P_\infty}{\rho} + \frac{1}{2}U_\infty^2 = \frac{P_{TE}^+}{\rho} + \frac{1}{2}(U_{TE}^+)^2 = \frac{P_{TE}^-}{\rho} + \frac{1}{2}(U_{TE}^-)^2 \quad (11.66)$$

$$\frac{P_{TE}^+}{\rho} = \frac{P_{TE}^-}{\rho} \quad (11.67)$$

$$U_{TE}^+ = U_{TE}^- \quad (11.68)$$

Conditions at the  
trailing edge



Define a disturbance potential

$$\Phi = U_{\infty}x\cos(\alpha) + U_{\infty}y\sin(\alpha) + \phi(x,y) \quad (11.69)$$

and disturbance velocities

$$\begin{aligned} U &= U_{\infty}\cos(\alpha) + u(x,y) \\ V &= U_{\infty}\sin(\alpha) + v(x,y) \end{aligned} \quad (11.70)$$

$$u = \frac{\partial\phi}{\partial x} \quad v = \frac{\partial\phi}{\partial y} \quad (11.71)$$

The disturbance potential satisfies Laplace's equation

$$\nabla^2\phi = 0 \quad (11.72)$$

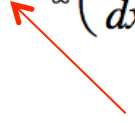
and goes to zero at infinity

$$\frac{\partial\phi}{\partial x} \rightarrow 0 \quad \frac{\partial\phi}{\partial y} \rightarrow 0 \quad \text{at } \infty \quad (11.73)$$

Nonlinear boundary conditions at the airfoil surface

$$v(x, f(x)) = \left. \frac{\partial \phi}{\partial y} \right|_{y=f(x)} = U_{\infty} \left( \frac{df}{dx} - \tan(\alpha) \right) \quad \text{on } 0 \leq x \leq C \quad (11.74)$$

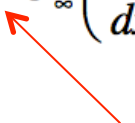
$$v(x, g(x)) = \left. \frac{\partial \phi}{\partial y} \right|_{y=g(x)} = -U_{\infty} \left( \frac{dg}{dx} - \tan(\alpha) \right) \quad \text{on } 0 \leq x \leq C . \quad (11.75)$$


+

Linearized boundary conditions applied at  $y=0$

$$v(x, 0^+) = \left. \frac{\partial \phi}{\partial y} \right|_{y=0^+} = U_{\infty} \left( \frac{df}{dx} - \alpha \right) \quad \text{on } 0 \leq x \leq C \quad (11.76)$$

$$v(x, 0^-) = \left. \frac{\partial \phi}{\partial y} \right|_{y=0^-} = -U_{\infty} \left( \frac{dg}{dx} - \alpha \right) \quad \text{on } 0 \leq x \leq C . \quad (11.77)$$


+

Define the thickness function

$$\eta_{Thickness}(x) = \frac{1}{2}(f(x) - g(x)) \quad (11.78)$$

Define the camber function

$$\eta_{Camber}(x) = \frac{1}{2}(f(x) + g(x)). \quad (11.79)$$

Linearized problem formulation

$$\nabla^2 \phi = 0$$

$$\lim_{r \rightarrow \infty} \frac{\partial \phi}{\partial x} = \lim_{r \rightarrow \infty} \frac{\partial \phi}{\partial y} = 0$$

$$\left. \frac{\partial \phi}{\partial y} \right|_{x,y=0^+} = U_{\infty} \frac{d\eta_{Thickness}}{dx} + U_{\infty} \frac{d\eta_{Camber}}{dx} - U_{\infty} \alpha \quad (11.80)$$

$$\left. \frac{\partial \phi}{\partial y} \right|_{x,y=0^-} = -U_{\infty} \frac{d\eta_{Thickness}}{dx} + U_{\infty} \frac{d\eta_{Camber}}{dx} - U_{\infty} \alpha$$

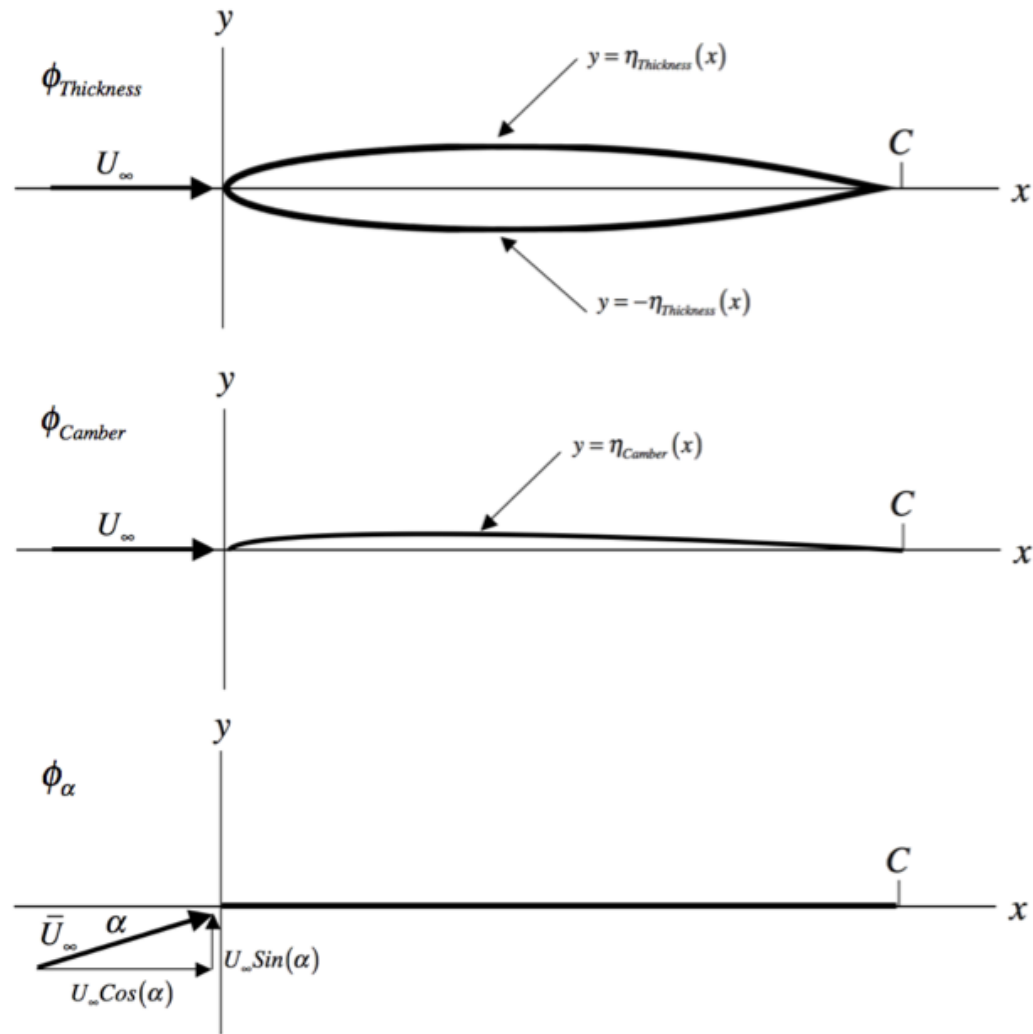


*Figure 11.12 The three basic problems of thin airfoil theory.*

$$\phi = \phi_{Thickness} + \phi_{Camber} + \phi_\alpha \quad (11.81)$$

### *The thickness problem*

Let the thickness disturbance field be represented by a distribution of mass sources along the  $x$ -axis in the range  $0 \leq x \leq C$ .

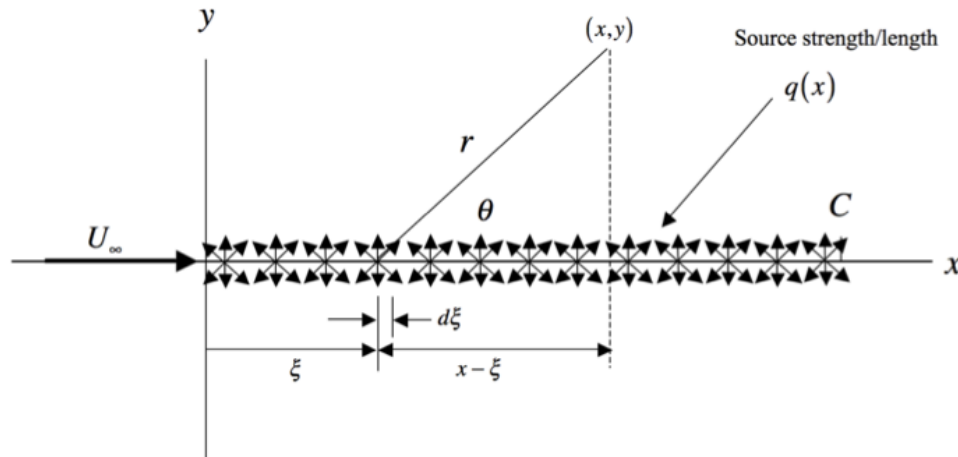


*Figure 11.13 Distribution of sources generating thickness.*

$$dW_{Thickness} = \frac{q(\xi)d\xi}{2\pi} \text{Ln}(re^{i\theta}) \quad (11.82)$$

$$r^2 = (x - \xi)^2 + y^2 \quad (11.83)$$

$$d\phi_{Thickness} = \frac{q(\xi)}{2\pi} \text{Ln}\left((x - \xi)^2 + y^2\right)^{1/2} d\xi \quad (11.84)$$

Contribution to the velocity potential from the thickness

$$\phi_{Thickness} = \frac{1}{2\pi} \int_0^c q(\xi) \text{Ln}((x - \xi)^2 + y^2)^{1/2} d\xi \quad (11.85)$$

Contribution to the velocity from the thickness

$$\begin{aligned} u_{Thickness}(x, y) &= \frac{\partial \phi_{Thickness}}{\partial x} = \frac{1}{2\pi} \int_0^c q(\xi) \frac{x - \xi}{(x - \xi)^2 + y^2} d\xi \\ v_{Thickness}(x, y) &= \frac{\partial \phi_{Thickness}}{\partial y} = \frac{1}{2\pi} \int_0^c q(\xi) \frac{y}{(x - \xi)^2 + y^2} d\xi \end{aligned} \quad (11.86)$$

Surface condition

$$\begin{aligned} v(x, 0^+) &= U_\infty \frac{d\eta_{Thickness}}{dx} \\ v(x, 0^-) &= -U_\infty \frac{d\eta_{Thickness}}{dx} \end{aligned} \quad (11.87)$$

We need to determine the source distribution that generates the correct surface condition. Let  $y = \varepsilon$

$$v_{Thickness}(x, \varepsilon) = \frac{1}{2\pi} \int_0^c q(\xi) \frac{\varepsilon}{(x - \xi)^2 + \varepsilon^2} d\xi \quad (11.88)$$

The entire contribution to this integral comes from the neighborhood of  $\xi = x$

This allows the source distribution to be pulled out of the integral.

$$v_{Thickness}(x, \varepsilon) = \frac{q(x)}{2\pi} \int_0^c \frac{\varepsilon}{(x - \xi)^2 + \varepsilon^2} d\xi \quad (11.89)$$

The integral can be evaluated.

$$\int_0^c \frac{\varepsilon}{(x - \xi)^2 + \varepsilon^2} d\xi = \int_0^{c/\varepsilon} \frac{1}{\left(\frac{x - \xi}{\varepsilon}\right)^2 + 1} d\left(\frac{\xi}{\varepsilon}\right) = \int_{\frac{x-C}{\varepsilon}}^{x/\varepsilon} \left(\frac{1}{\lambda^2 + 1}\right) d\lambda =$$

$$\text{ArcTan}\left(\frac{x}{\varepsilon}\right) - \text{ArcTan}\left(\frac{x-C}{\varepsilon}\right) \quad (11.90)$$

$$\lim_{\varepsilon \rightarrow 0} \left( \text{ArcTan}\left(\frac{x}{\varepsilon}\right) - \text{ArcTan}\left(\frac{x-C}{\varepsilon}\right) \right) = \pi$$

The distribution of source strength is now known in terms of the slope of the thickness distribution of the airfoil.

$$v_{Thickness}(x, 0^{\pm}) = \pm \frac{q(x)}{2} = \pm U_{\infty} \frac{d\eta_{Thickness}}{dx} . \quad (11.91)$$

$$q(x) = 2U_{\infty} \frac{d\eta_{thickness}}{dx} \quad (11.92)$$

The thickness potential is

$$\phi_{Thickness} = \frac{U_{\infty}}{2\pi} \int_0^c \frac{d\eta_{Thickness}(\xi)}{d\xi} \text{Ln}((x - \xi)^2 + y^2)^{1/2} d\xi . \quad (11.93)$$

Note that the total source strength is zero.

$$\int_0^c q(x) dx = \int_0^c U_{\infty} \frac{d\eta_{Thickness}}{dx} dx = U_{\infty} (\eta_{Thickness}(C) - \eta_{Thickness}(0)) = 0 \quad (11.94)$$



### *The camber problem*

Let the camber disturbance field be represented by a distribution of vortices along the  $x$ -axis in the range  $0 \leq x \leq C$ .

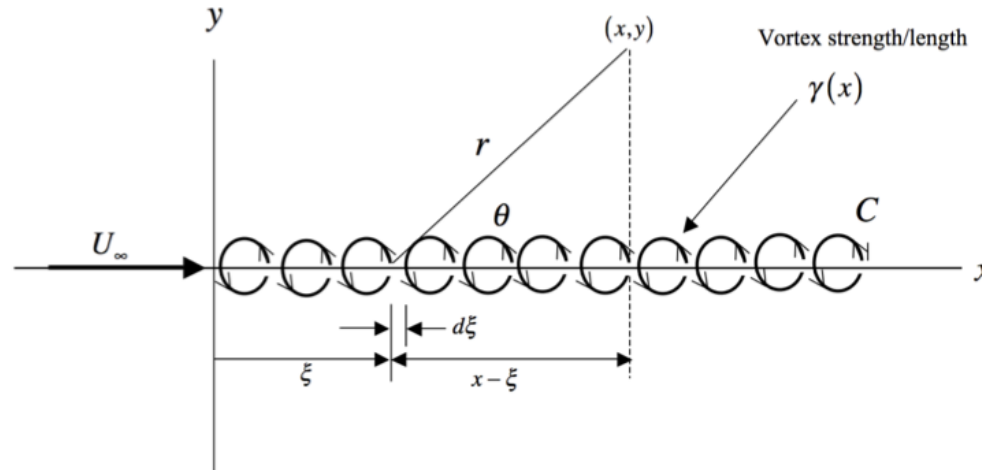


*Figure 11.14 Distribution of vortices generating camber.*

$$dW_{Camber} = \frac{\gamma(\xi)d\xi}{2\pi} iLn(re^{i\theta}) \quad (11.95)$$

$$r^2 = (x - \xi)^2 + y^2 \quad (11.96)$$

$$d\phi_{Camber} = -\frac{\gamma(\xi)}{2\pi} ArcTan\left(\frac{y}{x - \xi}\right) d\xi \quad (11.97)$$

Contribution to the velocity potential from the camber

$$\phi_{Camber} = -\frac{1}{2\pi} \int_0^c \gamma(\xi) \text{ArcTan}\left(\frac{y}{x-\xi}\right) d\xi \quad (11.98)$$

Contribution to the velocity from the camber

$$u_{Camber}(x,y) = \frac{\partial \phi_{Camber}}{\partial x} = \frac{1}{2\pi} \int_0^c \gamma(\xi) \frac{y}{(x-\xi)^2 + y^2} d\xi$$

$$v_{Camber}(x,y) = \frac{\partial \phi_{Camber}}{\partial y} = -\frac{1}{2\pi} \int_0^c \gamma(\xi) \frac{x-\xi}{(x-\xi)^2 + y^2} d\xi \quad (11.99)$$

Horizontal velocity component near the surface. Use the same procedure to pull the vortex source distribution out of the integral as was used for thickness.

$$u_{Camber}(x,0^\pm) = \lim_{y \rightarrow 0^\pm} \frac{1}{2\pi} \int_0^c \gamma(\xi) \frac{y}{(x-\xi)^2 + y^2} d\xi = \pm \frac{\gamma(x)}{2}. \quad (11.100)$$

Source strength is the circulation per unit length (the velocity jump) along the camber line.

$$\gamma(x) = u_{Camber}(x, 0^+) - u_{Camber}(x, 0^-) . \quad (11.101)$$

The surface condition for camber is.

$$v_{Camber}(x, 0^\pm) = \lim_{y \rightarrow 0^\pm} \left( -\frac{1}{2\pi} \int_0^c \gamma(\xi) \frac{x - \xi}{(x - \xi)^2 + y^2} d\xi \right) = U_\infty \frac{d\eta_{Camber}}{dx} . \quad (11.102)$$

Take the limit.

$$v_{Camber}(x, 0^\pm) = -\frac{1}{2\pi} \int_0^c \gamma(\xi) \frac{1}{(x - \xi)} d\xi = U_\infty \frac{d\eta_{Camber}}{dx} . \quad (11.103)$$

The pressure on the camber line is

$$P_\infty + \frac{1}{2} \rho U_\infty^2 = P_{Camber}(x, 0^\pm) + \frac{1}{2} \rho \left( (U_\infty + u_{Camber})^2 + (v_{Camber})^2 \right) \cong P_{Camber}(x, 0^\pm) + \frac{1}{2} \rho U_\infty^2 + \rho U_\infty u_{Camber}(x, 0^\pm) . \quad (11.104)$$

The lift due to camber is determined by the circulation due to camber

$$L = \int_0^c \left( P_{Camber} (x, 0^-) - P_{Camber} (x, 0^+) \right) dx . \quad (11.105)$$

$$L = \int_0^c \left( \rho U_\infty \frac{\gamma(x)}{2} + \rho U_\infty \frac{\gamma(x)}{2} \right) dx = \rho U_\infty \int_0^c \gamma(x) dx . \quad (11.106)$$

$$L = \rho U_\infty \Gamma$$

There is a moment about the leading edge due to camber

$$M = \int_0^c \left( P_{Camber} (x, 0^-) - P_{Camber} (x, 0^+) \right) x dx \quad (11.107)$$

$$M = \rho U_\infty \int_0^c \gamma(x) x dx . \quad (11.108)$$

But we still do not know  $\gamma(x)$

We need to solve

$$\int_0^C \frac{\gamma(\xi)}{x-\xi} d\xi = -2\pi U_\infty \frac{d\eta_{Camber}}{dx} \quad 0 \leq x \leq C \quad \gamma(C) = 0 . \quad (11.109)$$

1) Introduce

$$\begin{aligned} x &= \frac{C}{2}(1 + \cos(\theta)) \\ \xi &= \frac{C}{2}(1 + \cos(\zeta)) \end{aligned} . \quad (11.110)$$

This change of variables is illustrated below.

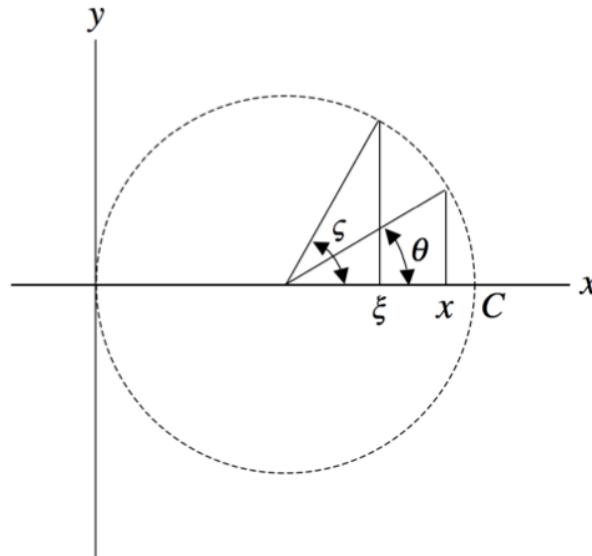


*Figure 11.15 The change of variables (11.110).*

2) Express  $\eta_{Camber}(x)$  as a Fourier series in  $\theta$ .

$$\frac{d\eta_{Camber}}{dx} = \sum_{n=0}^{\infty} B_n \text{Cos}(n\theta) \quad (11.111)$$

The coefficients are determined from the orthogonality of the expansion functions.

$$B_n = \frac{2}{\pi} \int_0^{\pi} \left( \frac{d\eta_{Camber}}{dx} \right) \text{Cos}(n\theta) d\theta \quad \text{for } n \geq 1, \quad B_0 = \frac{1}{\pi} \int_0^{\pi} \left( \frac{d\eta_{Camber}}{dx} \right) d\theta \quad (11.112)$$


---

3) Solve the integral (11.109) in the form

$$\frac{1}{2\pi U_{\infty}} \int_{\pi}^0 \frac{\gamma(\zeta)}{\text{Cos}(\zeta) - \text{Cos}(\theta)} d\zeta = \sum_{n=0}^{\infty} B_n \text{Cos}(n\theta) . \quad (11.113)$$

$$\gamma(\theta) = -2U_{\infty} \sum_{n=1}^{\infty} B_n \text{Sin}(n\theta) + 2 \frac{U_{\infty} B_0}{\text{Sin}(\theta)} \left( \frac{K}{2U_{\infty} B_0} + \text{Cos}(\theta) \right) . \quad (11.114)$$

The constant  $K$  is determined by the Kutta condition  $\gamma(\theta=0)=0$ . The result is  $K = -2U_\infty B_0$  which cancels the singularity at  $\theta = 0$  in (11.114). Thus

$$\gamma(\theta) = -2U_\infty \left( B_0 \left( \frac{1 - \cos(\theta)}{\sin(\theta)} \right) + \sum_{n=1}^{\infty} B_n \sin(n\theta) \right) . \quad (11.115)$$

Note that in general there is a singularity in the circulation at the leading edge where  $\theta = \pi$ .

The lift coefficient due to camber only depends on the first two coefficients in the series.

$$C_L = \frac{L}{\frac{1}{2}\rho U_\infty^2 C} = \frac{1}{U_\infty} \int_0^\pi \gamma(\theta) \sin(\theta) d\theta = -\pi(2B_0 + B_1) \quad (11.116)$$

The moment coefficient depends on the first three coefficients in the series.

$$\begin{aligned}
 C_M &= \frac{M}{\frac{1}{2}\rho U_\infty^2 C^2} = \frac{1}{2U_\infty} \int_0^\pi \gamma(\theta)(1 + \cos(\theta)) \sin(\theta) d\theta = \\
 &-\frac{\pi}{4}(2B_0 + B_1) - \frac{\pi}{4}(B_1 + B_2)
 \end{aligned} \quad (11.117)$$

The moment coefficient due to camber can be thought of as a pure moment or couple about the leading edge plus a moment due to lift acting at the 1/4 chord point.

$$C_M = \frac{C_L}{4} - \frac{\pi}{4}(B_1 + B_2). \quad (11.118)$$

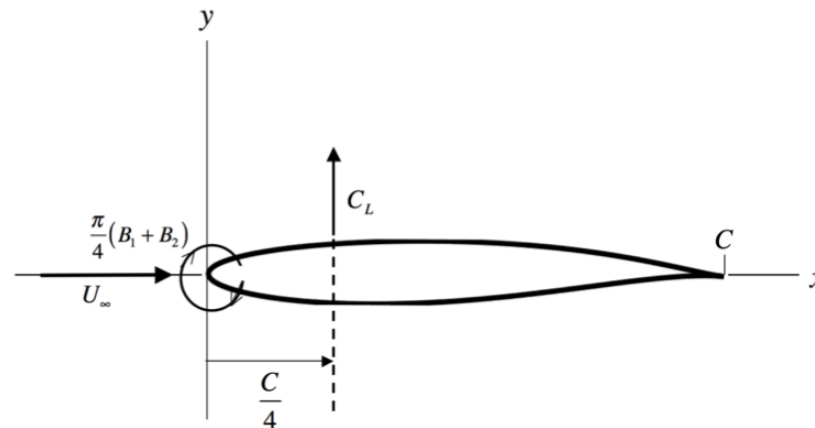


Figure 11.16 Forces and moments on a thin cambered airfoil at zero angle of attack.



### The angle-of-attack problem

Finally we look at the incompressible potential flow past a flat plate at a small angle of attack illustrated below. The source is modeled as a distribution of vortices as in the camber problem.

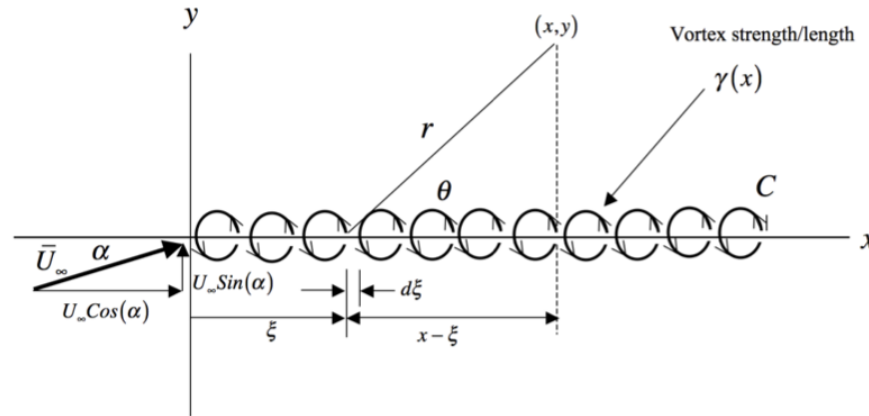


Figure 11.17 Distribution of vortices generating lift on a flat plate at angle-of-attack  $\alpha$ .

In this case the surface condition is especially simple since  $d\eta_{Camber} / dx = -\alpha$ .

$$v_{Camber}(x, 0^\pm) = -U_\infty \alpha \quad (11.119)$$

$$\int_0^C \frac{\gamma(\xi)}{x - \xi} d\xi = 2\pi U_\infty \alpha \quad 0 \leq x \leq C \quad \gamma(C) = 0. \quad (11.120)$$

$$B_0 = -\frac{1}{\pi} \int_0^\pi \alpha d\theta = -\alpha, \quad B_1, B_2, B_3, \dots, B_n = 0 \quad (11.121)$$

Potential flow for a flat plate at an angle of attack in low speed flow.

$$\gamma(\theta) = 2U_{\infty}\alpha \left( \frac{1 - \cos(\theta)}{\sin(\theta)} \right). \quad (11.122)$$

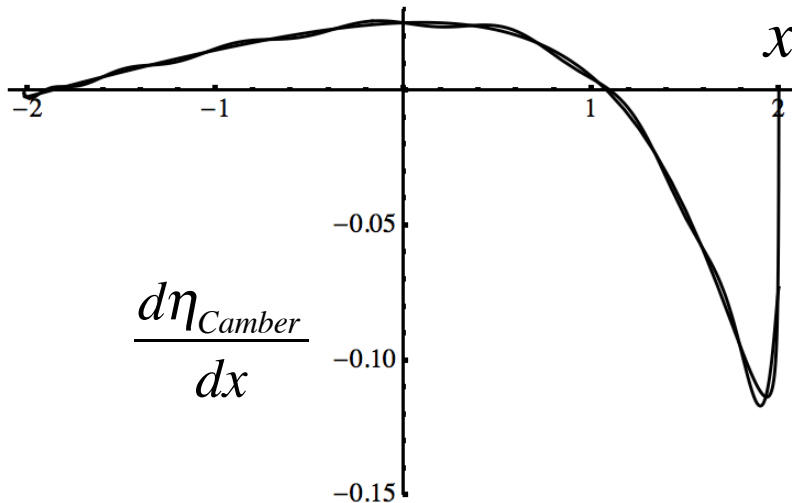
$$C_L = 2\pi\alpha$$

$$C_M = \frac{\pi}{2}\alpha. \quad (11.123)$$

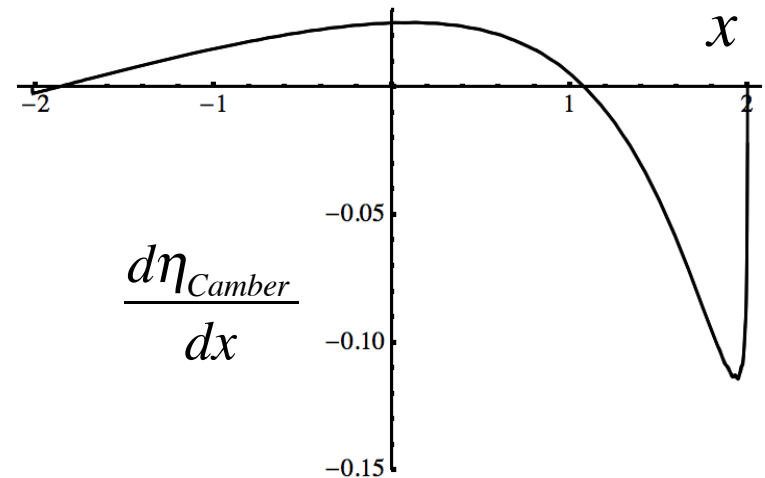
# Convergence of the series approximating the camber function

$$\frac{d\eta_{Camber}}{dx} = \sum_{n=0}^{\infty} B_n \cos(n\theta) \quad (11.111)$$

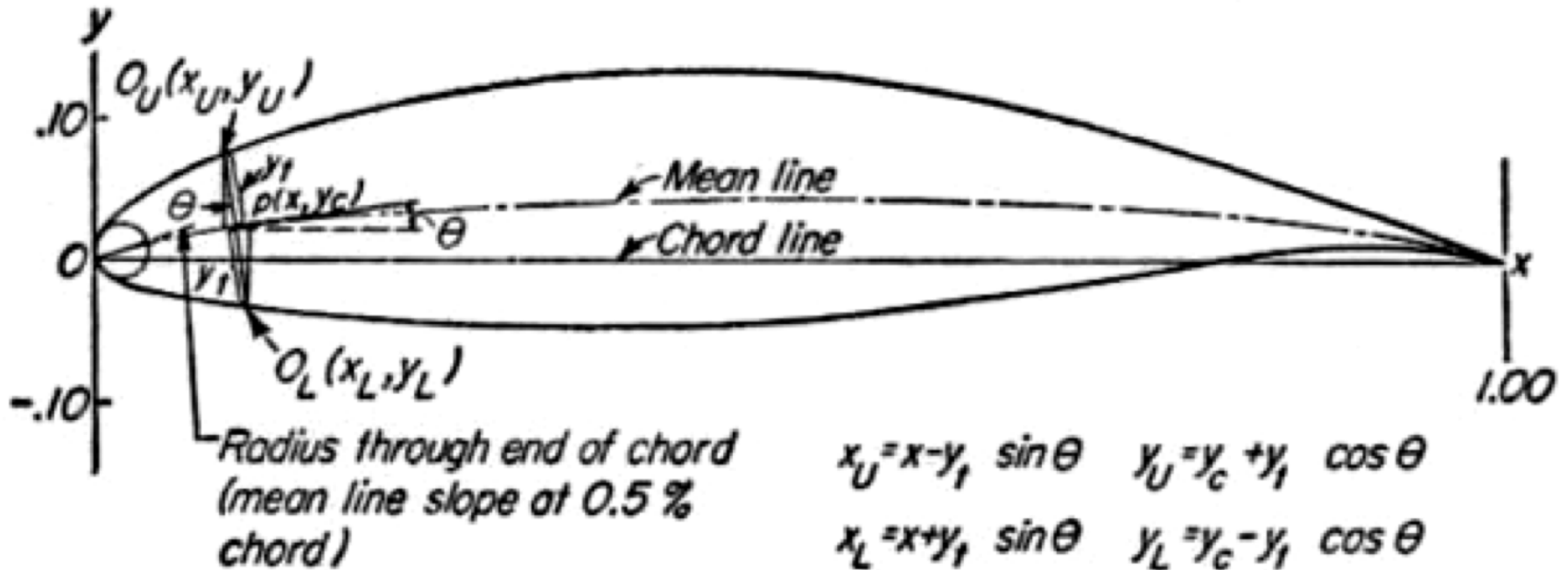
n=16



n=100



## NACA airfoil numbering system



## NACA airfoil geometrical construction

## NACA Four-Digit Series:

The first family of airfoils designed using this approach became known as the NACA Four-Digit Series. The first digit specifies the maximum camber ( $m$ ) in percentage of the chord (airfoil length), the second indicates the position of the maximum camber ( $p$ ) in tenths of chord, and the last two numbers provide the maximum thickness ( $t$ ) of the airfoil in percentage of chord. For example, the NACA 2415 airfoil has a maximum thickness of 15% with a camber of 2% located 40% back from the airfoil leading edge (or  $0.4c$ ). Utilizing these  $m$ ,  $p$ , and  $t$  values, we can compute the coordinates for an entire airfoil using the following relationships:

1. Pick values of  $x$  from 0 to the maximum chord  $c$ .
2. Compute the mean camber line coordinates by plugging the values of  $m$  and  $p$  into the following equations for each of the  $x$  coordinates.

$$y_c = \frac{m}{p^2}(2px - x^2) \quad \text{from } x = 0 \text{ to } x = p$$

$$y_c = \frac{m}{(1-p)^2}[(1-2p) + 2px - x^2] \quad \text{from } x = p \text{ to } x = c$$

where

$x$  = coordinates along the length of the airfoil, from 0 to  $c$  (which stands for chord, or length)

$y$  = coordinates above and below the line extending along the length of the airfoil, these are either  $y_t$  for thickness coordinates or  $y_c$  for camber coordinates

$t$  = maximum airfoil thickness in tenths of chord (i.e. a 15% thick airfoil would be 0.15)

$m$  = maximum camber in tenths of the chord

$p$  = position of the maximum camber along the chord in tenths of chord

3. Calculate the thickness distribution above (+) and below (-) the mean line by plugging the value of  $t$  into the following equation for each of the  $x$  coordinates.

$$\pm y_t = \frac{t}{0.2} (0.2969\sqrt{x} - 0.1260x - 0.3516x^2 + 0.2843x^3 - 0.1015x^4)$$

4. Determine the final coordinates for the airfoil upper surface ( $x_U, y_U$ ) and lower surface ( $x_L, y_L$ ) using the following relationships.

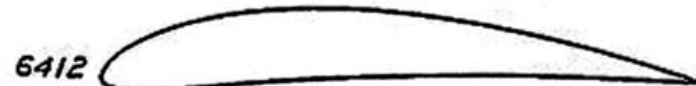
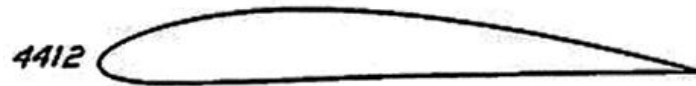
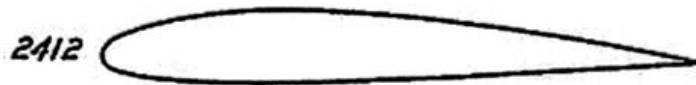
$$x_U = x - y_t \sin \theta$$

$$y_U = y_c + y_t \cos \theta$$

$$x_L = x + y_t \sin \theta$$

$$y_L = y_c - y_t \cos \theta$$

$$\text{where } \theta = \arctan\left(\frac{dy_c}{dx}\right)$$



### **NACA Five-Digit Series:**

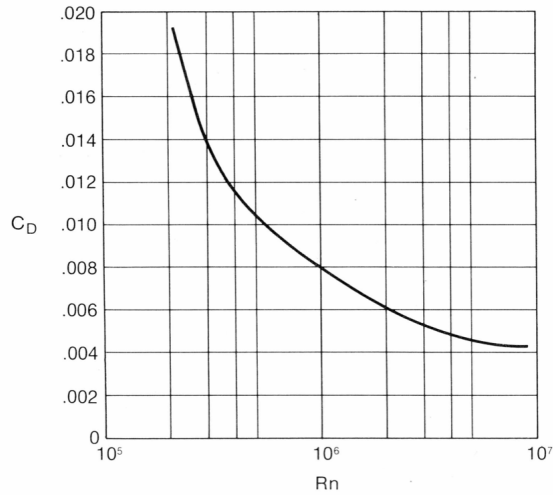
The NACA Five-Digit Series uses the same thickness forms as the Four-Digit Series but the mean camber line is defined differently and the naming convention is a bit more complex. The first digit, when multiplied by  $3/2$ , yields the design lift coefficient ( $c_l$ ) in tenths. The next two digits, when divided by 2, give the position of the maximum camber ( $p$ ) in tenths of chord. The final two digits again indicate the maximum thickness ( $t$ ) in percentage of chord. For example, the NACA 23012 has a maximum thickness of 12%, a design lift coefficient of 0.3, and a maximum camber located 15% back from the leading edge. The steps needed to calculate the coordinates of such an airfoil are:

and so on .....

Family	Advantages	Disadvantages	Applications
4-Digit	<ol style="list-style-type: none"> <li>1. Good stall characteristics</li> <li>2. Small center of pressure movement across large speed range</li> <li>3. Roughness has little effect</li> </ol>	<ol style="list-style-type: none"> <li>1. Low maximum lift coefficient</li> <li>2. Relatively high drag</li> <li>3. High pitching moment</li> </ol>	<ol style="list-style-type: none"> <li>1. General aviation</li> <li>2. Horizontal tails</li> </ol> <p><b>Symmetrical:</b></p> <ol style="list-style-type: none"> <li>3. Supersonic jets</li> <li>4. Helicopter blades</li> <li>5. Shrouds</li> <li>6. Missile/rocket fins</li> </ol>
5-Digit	<ol style="list-style-type: none"> <li>1. Higher maximum lift coefficient</li> <li>2. Low pitching moment</li> <li>3. Roughness has little effect</li> </ol>	<ol style="list-style-type: none"> <li>1. Poor stall behavior</li> <li>2. Relatively high drag</li> </ol>	<ol style="list-style-type: none"> <li>1. General aviation</li> <li>2. Piston-powered bombers, transports</li> <li>3. Commuters</li> <li>4. Business jets</li> </ol>
16-Series	<ol style="list-style-type: none"> <li>1. Avoids low pressure peaks</li> <li>2. Low drag at high speed</li> </ol>	<ol style="list-style-type: none"> <li>1. Relatively low lift</li> </ol>	<ol style="list-style-type: none"> <li>1. Aircraft propellers</li> <li>2. Ship propellers</li> </ol>
6-Series	<ol style="list-style-type: none"> <li>1. High maximum lift coefficient</li> <li>2. Very low drag over a small range of operating conditions</li> <li>3. Optimized for high speed</li> </ol>	<ol style="list-style-type: none"> <li>1. High drag outside of the optimum range of operating conditions</li> <li>2. High pitching moment</li> <li>3. Poor stall behavior</li> <li>4. Very susceptible to roughness</li> </ol>	<ol style="list-style-type: none"> <li>1. Piston-powered fighters</li> <li>2. Business jets</li> <li>3. Jet trainers</li> <li>4. Supersonic jets</li> </ol>
7-Series	<ol style="list-style-type: none"> <li>1. Very low drag over a small range of operating conditions</li> <li>2. Low pitching moment</li> </ol>	<ol style="list-style-type: none"> <li>1. Reduced maximum lift coefficient</li> <li>2. High drag outside of the optimum range of operating conditions</li> <li>3. Poor stall behavior</li> <li>4. Very susceptible to roughness</li> </ol>	Seldom used
8-Series	Unknown	Unknown	Very seldom used



# Viscous effects - from *Wing Theory* by R.T. Jones



3.14. Variation of minimum drag coefficient with Reynolds number, NACA 65-418 airfoil.

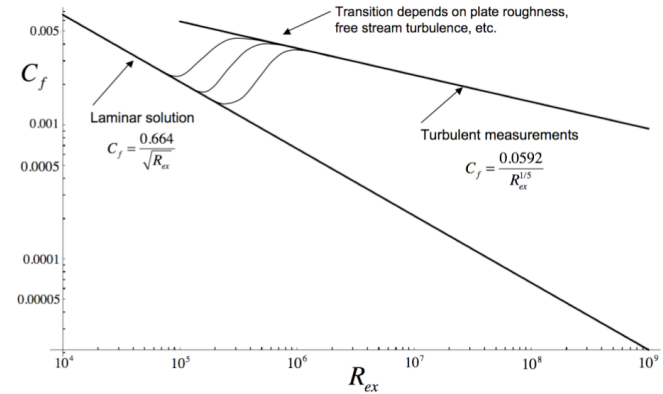
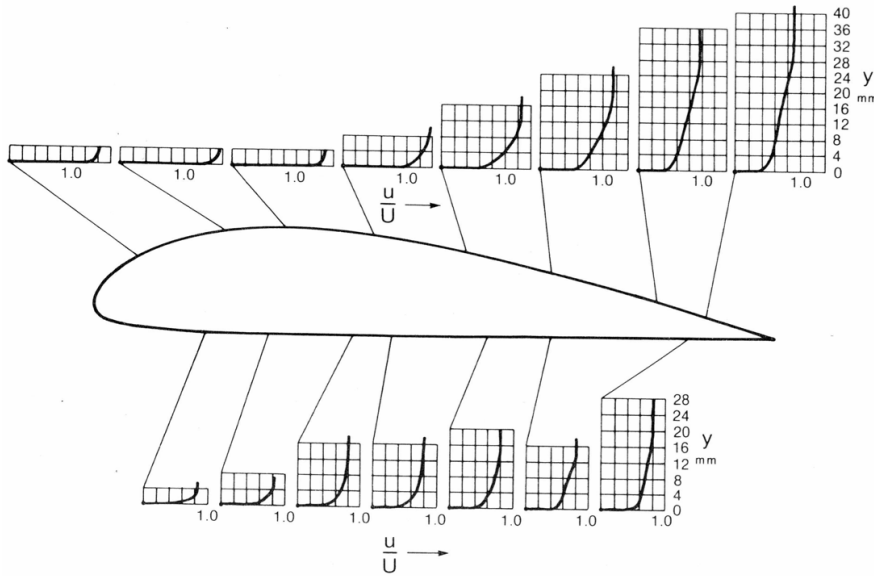
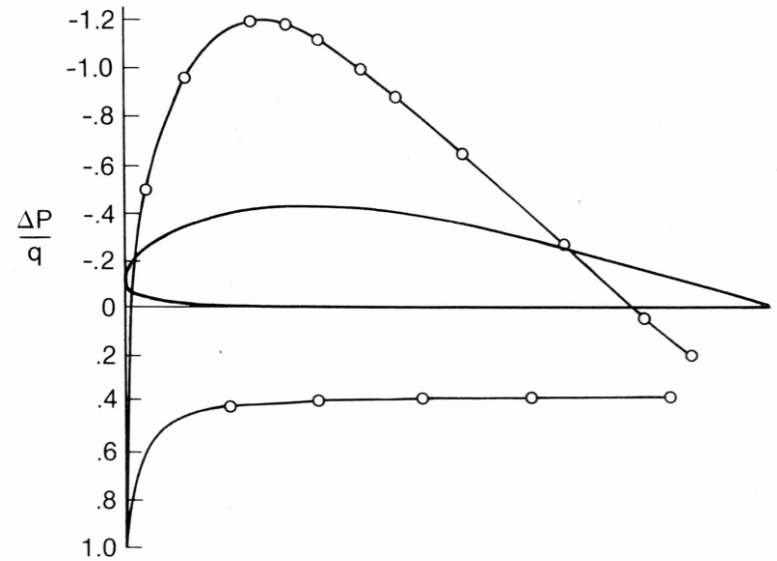


Figure 8.11 Friction coefficient for incompressible flow on a flat plate.

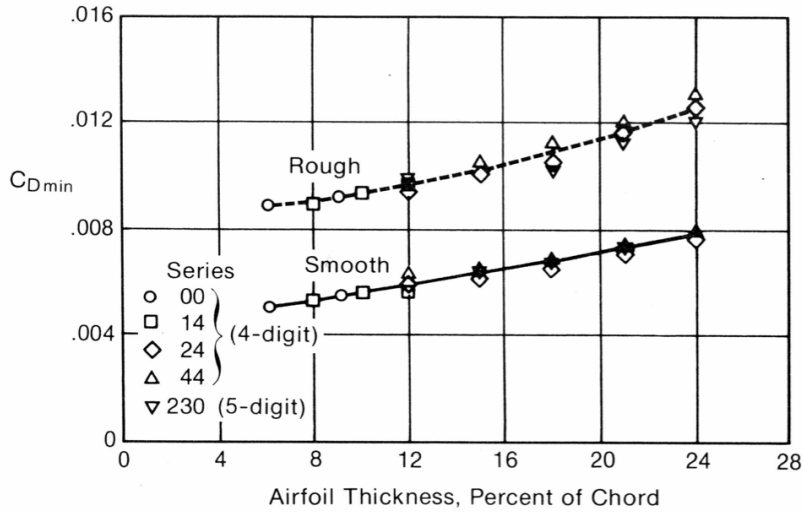


3.15a. Boundary layer profiles measured in flight.



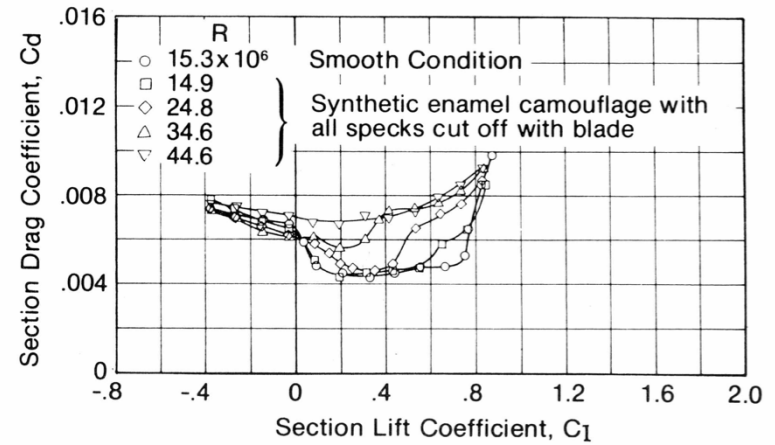
3.15b. Pressure distribution, G-387 airfoil.

## Roughness effects



3.16. Variation of profile drag with thickness and surface condition.

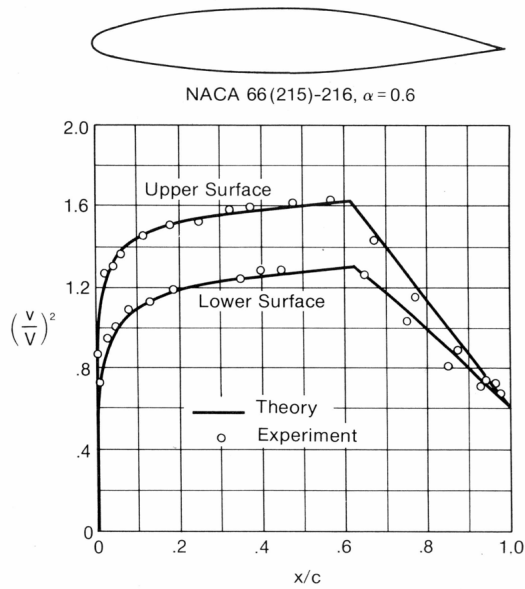
Roughness consisted of a strip of 0.01 inch  
Carborundum grains near the airfoil leading edge.



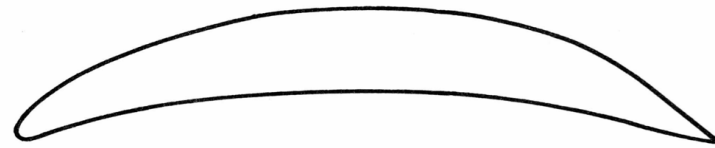
3.17. Drag characteristics of NACA 65(421)-420 airfoil for two surface conditions.

Roughness consisted of a coat of camouflage paint.

## Efforts at Drag control



3.12. Comparison of theoretical and experimental pressure distributions for NACA laminar flow airfoil.



3.18. NACA 27-2012 airfoil:  $C_l = 1.78$ ,  $C_d = .0061$ ,  $L/D = 292$ ,  $R = 2.3 \times 10^6$ .

A record setter

# An experimental flow with zero skin friction throughout its region of pressure rise

By B. S. STRATFORD

National Gas Turbine Establishment, Farnborough

(Received 17 July 1958)

A flow has been produced having effectively zero skin friction throughout its region of pressure rise, which extended for a distance of 3 ft. No fundamental difficulty was encountered in establishing the flow and it had, moreover, a good margin of stability. The dynamic head in the zero skin friction boundary layer was found to be linear at the wall (i.e.  $u \propto y^{\frac{1}{2}}$ ), as predicted theoretically in the previous paper (Stratford 1959).

The flow appears to achieve any specified pressure rise in the shortest possible distance and with probably the least possible dissipation of energy for a given initial boundary layer. Thus an aerofoil which could utilize it immediately after transition from laminar flow would be expected to have a very low drag. A design pressure distribution (besides having the usual safety margin against stall) should have a slightly more gradual start to the pressure rise than in the present experiment, as small errors close to the discontinuity can cause difficulty.

*JFM Vol 5*

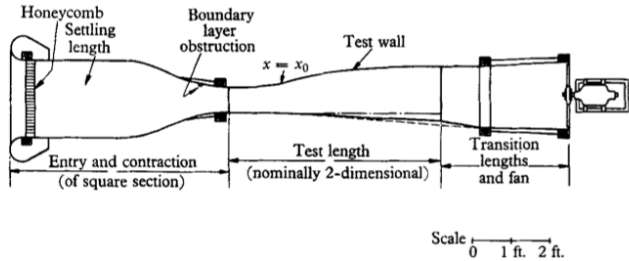


FIGURE 1. Plan-section sketch of the wind tunnel.

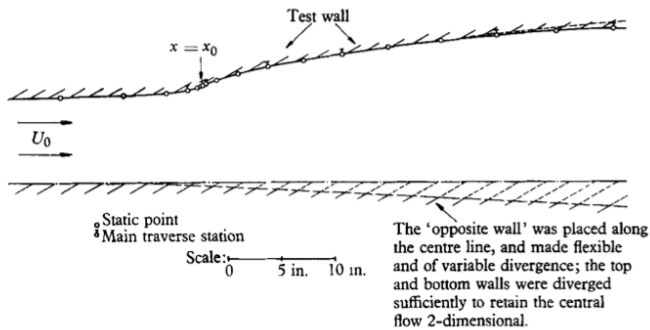


FIGURE 2. Design of the test section.

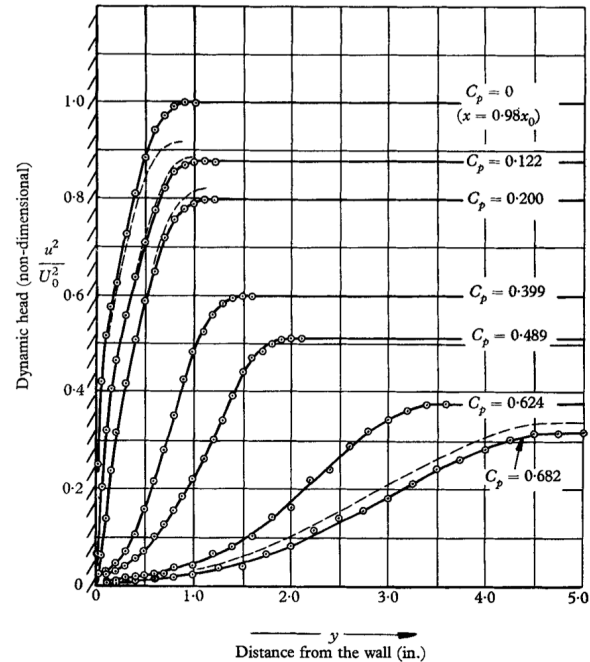
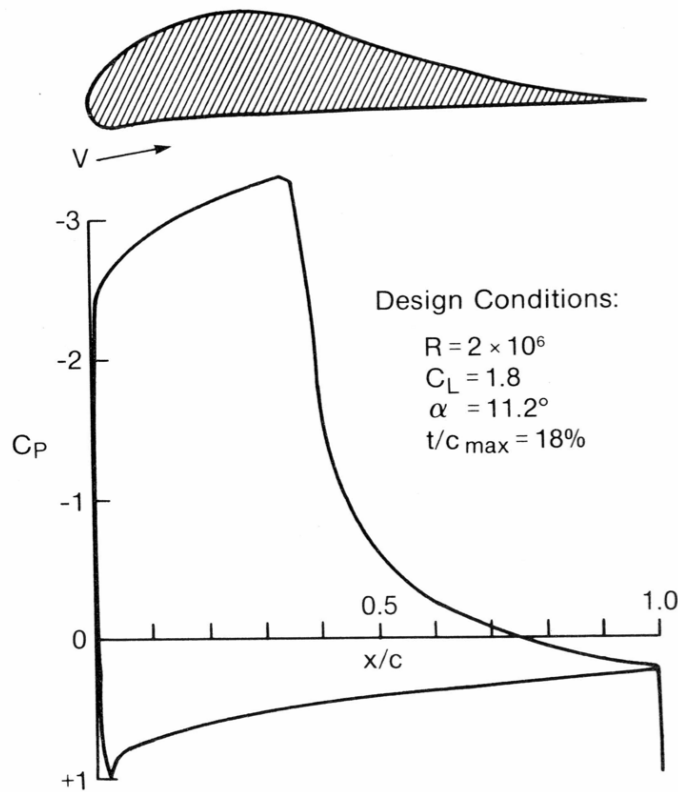
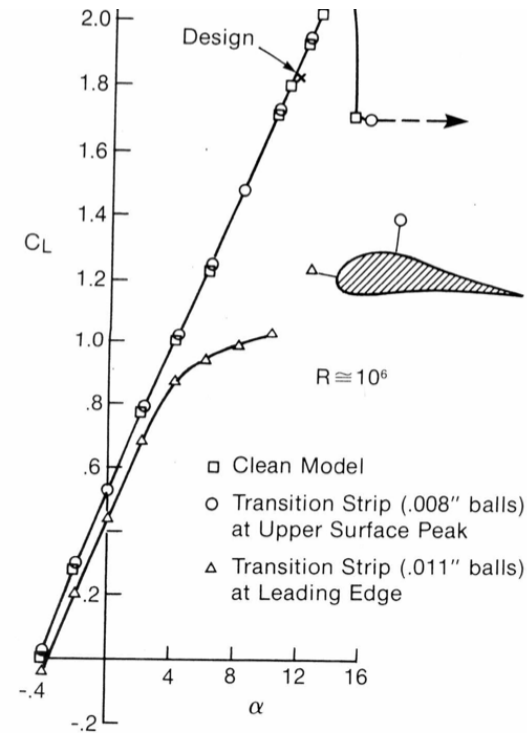


FIGURE 3. The dynamic head profiles. The full line profiles represent total pressure minus static pressure at the wall. Where the static pressure varies across the boundary layer the true dynamic head is represented by the broken lines. The  $C_p$  values refer to the wall.

## Effort to maintain incipient separation



3.19a. Laminar rooftop airfoil, geometry and pressure distribution.



3.19b. Laminar rooftop airfoil, lift curves showing the effect of transition strips. (From R. H. Liebeck, "Wind Tunnel Tests of Two Airfoils Designed for High Lift without Separation in Incompressible Flow," Rep. MDC-J5667/01, McDonnell Douglas Aircraft Co., Aug. 1972. With permission of the author.)

¶

Read: Chapters 12 and 13

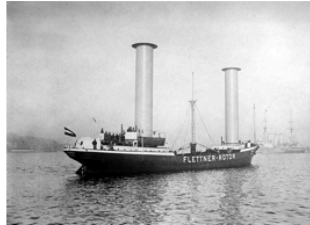
¶

**Problem 1** – Take the 2-D wing you studied in Homework 6 and use it as the cross-section of an elliptical planform 3-D wing with aspect ratio 10. Determine the lift, skin friction drag, induced drag and moment coefficients of the wing for several angles of attack. Ignore possible cross-flow effects.

**Problem 2** – Estimate the effect on the pressure distribution, lift and drag if the wing in problem 1 is flown at a Mach number of 0.5.

LAST YEAR'S SECOND EXAM

**Problem 3** – The figures below depict an innovative system for drawing propulsion from the wind developed by Anton Flettner in the 1920's. A motor below decks is used to turn a spinning cylinder. In the presence of the wind a force acts on the cylinder. The force can be used to supplement the thrust of the ship's propellers. With proper design the system can be more efficient than one where all the power is applied to the ship's propellers. Both Jacob Ackeret (a swiss aerodynamicist) and Ludwig Prandtl helped Flettner with his design.



1) The original concept shown in the left figure used two cylinders each 15 meters high and 3 meters in diameter driven by 40 kilowatt motors turning the cylinders at 0.25 revolutions per second. Estimate the force produced by each rotor in a 20 meter per second wind. The density of air at sea level is  $1.225 \text{ kg} / \text{m}^3$ .

2) What is the role of viscosity in this concept? To help you think about this problem suppose a cylinder is set into rotation at a constant frequency in a viscous incompressible fluid initially at rest. After a short period a slowly changing velocity field near the cylinder is established. Sketch the velocity profile.

**Problem 4** – A solar powered light aircraft with a rectangular wing is designed for flight at low speed at an altitude of 5,000 meters (air density  $0.74 \text{ kg} / \text{m}^3$ ). The drag coefficient is

$$C_D = C_{Dp} + \frac{C_L^2}{\pi \epsilon_0} \frac{S}{b^2}$$

where the coefficient of profile drag is  $C_{Dp} = 0.01$  and the Oswald efficiency is  $\epsilon_0 = 0.8$ . The wing span is 15 meters and the wing chord is 1 meter. The aircraft mass including the pilot is 180 kg. Determine the flight speed  $U_\infty$  that minimizes the drag.

**Problem 5** – The lift coefficient on a thin 2D wing spanning a wind tunnel is measured to be 0.55 at a free stream Mach number of 0.4. The wing is rotated to a sweep angle of 60 degrees and the Mach number of the flow is increased to 1.5. Estimate the lift coefficient of the swept wing.